Downloaded from genome.cshlp.org on June 12, 2026 . Published by Cold Spring Harbor Laboratory Press

The genome of the colonial hydroid *Hydractinia* reveals their stem cells utilize a toolkit of evolutionarily shared genes with all animals

Christine E. Schnitzler, E. Sally Chang, Justin Waletich, et al.

Genome Res. published online March 20, 2024
Access the most recent version at doi:10.1101/gr.278382.123

P<P Published online March 20, 2024 in advance of the print journal.

Accepted Manuscript Peer-reviewed and accepted for publication but not copyedited or typeset; accepted manuscript is likely to differ from the final, published version.

Open Access Freely available online through the *Genome Research* Open Access option.

Creative Commons License This manuscript is Open Access.This article, published in *Genome Research*, is available under a Creative Commons License (Attribution 4.0 International license), as described at http://creativecommons.org/licenses/by/4.0/.

Email Alerting Service Receive free email alerts when new articles cite this article - sign up in the box at the top right corner of the article or **click here.**

To subscribe to *Genome Research* go to:
https://genome.cshlp.org/subscriptions

Published by Cold Spring Harbor Laboratory Press

Downloaded from genome.cshlp.org on June 12, 2026 . Published by Cold Spring Harbor Laboratory Press

The genome of the colonial hydroid Hydractinia reveals their stem cells utilize a toolkit of evolutionarily shared genes with all animals

Christine E. Schnitzler[1,2], E. Sally Chang[3,4], Justin Waletich[1,2], Gonzalo Quiroga-Artigas[1,2,5], Wai Yee Wong[6], Anh-Dao Nguyen[3], Sofia N. Barreira[3], Liam B. Doonan[7], Paul Gonzalez[3], Sergey Koren[3], James M. Gahan[7,8], Steven M. Sanders[9,10], Brian Bradshaw[7], Timothy Q. DuBuc[7,11], Febrimarsa[7,12], Danielle de Jong[1,2], Eric P. Nawrocki[4], Alexandra Larson[1], Samantha Klasfeld[3], Sebastian G. Gornik[7,13], R. Travis Moreland[3], Tyra G. Wolfsberg[3], Adam M. Phillippy[3], James C. Mullikin[3,14], Oleg Simakov[6], Paulyn Cartwright[15], Matthew Nicotra[9,10], Uri Frank[7], Andreas D. Baxevanis[3]

[1]Whitney Laboratory for Marine Bioscience, University of Florida, St. Augustine, FL 32080, USA; [2]Department of Biology, University of Florida, Gainesville, FL 32611, USA; [3]Division of Intramural Research, National Human Genome Research Institute, National Institutes of Health, Bethesda, MD 20892, USA; [4]National Center for Biotechnology Information, National Library of Medicine, National Institutes of Health, Bethesda, MD 20892, USA; [5]Centre de Recherche en Biologie cellulaire de Montpellier (CRBM), Université de Montpellier, Centre National de la Recherche Scientifique, 34293 Montpellier CEDEX 05, France; [6]Department for Neurosciences and Developmental Biology, University of Vienna, 1030 Vienna, Austria; [7]Centre for Chromosome Biology, College of Science and Engineering, University of Galway, Galway, Ireland; [8]Department of Biochemistry, University of Oxford, Oxford, UK; [9]Department of Surgery, Thomas E. Starzl Transplantation Institute, University of Pittsburgh, Pittsburgh, PA 15261, USA; [10]Pittsburgh Center for Evolutionary Biology and Medicine, University of Pittsburgh, Pittsburgh, PA 15261, USA; [11]Swarthmore College, Swarthmore, PA 19081, USA; [12]Pharmaceutical Biology Lab, Faculty of Pharmacy, Universitas Muhammadiyah Surakarta, Jawa Tengah, Indonesia; [13]Centre for Organismal Studies, University of Heidelberg, Germany; [14]NIH

Downloaded from genome.cshlp.org on June 12, 2026 . Published by Cold Spring Harbor Laboratory Press

Intramural Sequencing Center, Rockville, MD 20852, USA; [15]Department of Evolution and Ecology, University of Kansas, Lawrence, KS 66045, USA

ABSTRACT

Hydractinia is a colonial marine hydroid that exhibits remarkable biological properties, including the capacity to regenerate its entire body throughout its lifetime, a process made possible by its adult migratory stem cells, known as i-cells. Here, we provide an in-depth characterization of the genomic structure and gene content of two *Hydractinia* species, *H. symbiolongicarpus* and *H. echinata*, placing them in a comparative evolutionary framework with other cnidarian genomes. We also generated and annotated a single-cell transcriptomic atlas for adult male *H. symbiolongicarpus* and identified cell type markers for all major cell types, including key i-cell markers. Orthology analyses based on the markers revealed that *Hydractinia*'s i-cells are highly enriched in genes that are widely shared amongst animals, a striking finding given that *Hydractinia* has a higher proportion of phylum-specific genes than any of the other 41 animals in our orthology analysis. These results indicate that *Hydractinia*'s stem cells and early progenitor cells may use a toolkit shared with all animals, making it a promising model organism for future exploration of stem cell biology and regenerative medicine. The genomic and transcriptomic resources for *Hydractinia* presented here will enable further studies of their regenerative capacity, colonial morphology, and ability to distinguish self from non-self.

INTRODUCTION

The increasing number of genome sequences that are now available for non-bilaterian animal species has provided a strong foundation for better understanding the molecular innovations that drove the surge of diversity seen in early animal evolution. Of particular interest are the

Downloaded from genome.cshlp.org on June 12, 2026 . Published by Cold Spring Harbor Laboratory Press

cnidarians, a phylum comprised of over 10,000 species that include the corals, sea anemones, jellyfish, and hydroids (Steele et al. 2011, Gahan et al. 2023). The distinguishing feature that unifies all members of this phylum is that they possess a specialized type of stinging cell called a cnidocyte that is used to both ward off enemies and capture prey. From a genomic standpoint, the cnidarians occupy an informative position on the animal tree as the sister group to the bilaterians, making them a powerful model for studying numerous biological processes common to all animals. From a biomedical standpoint, they have been found to encode more orthologs to genes associated with human disease than do classic invertebrate models, supporting the proposition that they can serve as viable models for studying various classes of human diseases (Maxwell 2014).

One particular cnidarian species that has already proven to be an excellent model for the study of questions regarding stem cells, regeneration, allorecognition, and coloniality is *Hydractinia,* a small colonial marine invertebrate that grows on snail shells inhabited by hermit crabs. The polyp types found within these gonochoristic colonies include feeding polyps (gastrozooids) that feed opportunistically on small plankton and share resources throughout the colony, sexual polyps (gonozooids), and defensive polyps (dactylozooids and tentaculozooids). The colonies lend themselves to experimental study as they are easily cultured on glass microscope slides (Fig. 1A). Marine hydroids, including *Hydractinia*, have fascinated biologists since the late 1800s (Weismann 1883) due to their population of pluripotent stem cells, called ‘i-cells’ due to their localization within the interstitial spaces of its epithelial cells (Varley et al. 2023); these i-cells are responsible for *Hydractinia*’s remarkable regenerative capabilities. In fact, the term ‘stem cell’ (*stamzellen*) was coined by August Weismann in an 1883 chapter on *Hydractinia*’s putative migratory sperm progenitors (Weismann 1883; Wessel 2013). Additional characteristics of these organisms such as allorecognition – a colony’s ability to distinguish itself from conspecifics – have also received considerable attention (Nicotra 2019). Their closest well-studied relative is

Downloaded from genome.cshlp.org on June 12, 2026 . Published by Cold Spring Harbor Laboratory Press

the freshwater *Hydra* that shares many characteristics with *Hydractinia*, including possessing i-cells, the capacity for whole-body regeneration, and the absence of a medusa adult phase. However, *Hydractinia* differs from *Hydra* in several important respects, including its colonial morphology, polyp polymorphism, and possession of a single self-renewing stem cell lineage (Varley et al. 2023), as compared to the three self-renewing lineages found in *Hydra* (interstitial, endodermal, and ectodermal). There are also salient differences in their life cycles, with *Hydractinia* undergoing metamorphosis from the larval to adult form, whereas *Hydra* exhibits direct development with no larval stage. These differences between the two lineages are unsurprising given that they diverged at least 500 MYA (Steele et al. 2011).

Here, we report highly contiguous genome assemblies for two species: *H. symbiolongicarpus*, found along the east coast of the United States, and *H. echinata*, found in European waters, comparing their genome structure and content with those of other cnidarians and other animals. These whole-genome sequence data have served as the basis for performing several evolutionary analyses, including ortholog clustering based on the predicted proteomes from 49 species that encompass a wide array of animals and unicellular eukaryotes, as well as analyses aimed at deducing lineage-specific evolutionary novelties. Orthology inference analyses allowed for a thorough description of overall gene evolutionary patterns, including lineage specificity and gene family dynamics.

In addition to identifying the homeobox gene complement of *Hydractinia*, we also report the first comprehensive description of the non-coding RNA (ncRNA) landscape of any cnidarian species. Finally, we have employed a single-cell transcriptomic approach to create a robust cell-type atlas for *H. symbiolongicarpus* that has allowed for the identification of several known cell types and cell states, including two clusters with distinct stem cell (‘i-cell’) signatures. Our study provides evidence that, despite the level of evolutionary novelty observed within cnidarians (and

Downloaded from genome.cshlp.org on June 12, 2026 . Published by Cold Spring Harbor Laboratory Press

particularly within the *Hydractinia* genomes themselves), i-cells express a set of evolutionary conserved genes that are found throughout the animal tree, a finding that may have broader implications for our understanding of stem cell and regenerative biology.

RESULTS

Sequencing, assembly, and annotation of *Hydractinia* genomes

We estimated the genome sizes for *Hydractinia symbiolongicarpus* male wild-type strain 291-10, *Hydractinia echinata* female wild-type strain F4, the closely related hydrozoan *Podocoryna carnea* male wild-type strain PcLH01, and *Hydra vulgaris* strain 105 using propidium iodide staining of isolated nuclei followed by flow cytometric analysis (Hare and Johnston 2011) (for details, see Supplemental Material). The resulting genome size estimates were 514 Mb for *H. symbiolongicarpus* and 775 Mb for *H. echinata* (Supplemental Table S1). By way of comparison, our estimate for *P. carnea* was 517 Mb and 1086 Mb for *H. vulgaris*, consistent with previous reports (Chapman et al. 2010). We then isolated high molecular weight DNA from adult polyps and sequenced both *Hydractinia* genomes using a combination of PacBio SMRT long-read and Illumina short-read sequence data (for details, see Supplemental Material; Supplemental Table S2). These PacBio data were then used to generate primary contig assemblies using the diploid-aware assembler Canu (Koren et al. 2017) (Supplemental Tables S3, S4). Canu attempts to assemble and phase contigs representing alternative haplotypes in heterozygous regions into primary and secondary assemblies via a filtering step, but this phasing can be challenging when applied to genomes that exhibit a high level of heterozygosity. Here, we estimated overall heterozygosity to be 1.33% for *H. symbiolongicarpus* and 0.85% for *H. echinata* (Supplemental Fig. S1). In addition, Canu phasing resulted in primary assemblies that had many duplicated loci, with initial BUSCO (Simão et al. 2015) analyses indicating 42%

Downloaded from genome.cshlp.org on June 12, 2026 . Published by Cold Spring Harbor Laboratory Press

and 29% duplicated genes in the *H. symbiolongicarpus* and *H. echinata* assemblies, respectively. To address this, we used MUMmer 3.23 (Kurtz et al. 2004) to better-separate haplotypes (for details, see Supplemental Material). Following this contig filtering procedure, the presence of duplicated loci in the primary assemblies was reduced to 11% for *H. symbiolongicarpus* and 10% for *H. echinata*. These primary contig assemblies were then scaffolded with Illumina Chicago libraries through Dovetail HiRise scaffolding (Putnam et al. 2016), then gap-filled using PBJelly (English et al. 2012). The assemblies were polished using the final consensus-calling algorithm Arrow (Chin et al. 2013) and further polished with Pilon (Walker et al. 2014). The resulting final scaffolded and polished primary assemblies resulted in a 406 Mb assembly for *H. symbiolongicarpus* consisting of 4,840 scaffolds with a scaffold N50 of 2,236 kb, and a 565 Mb assembly for *H. echinata* consisting of 7,767 scaffolds with a scaffold N50 of 904 kb (Supplemental Table S3). The discrepancy between the final assembly sizes and the estimated genome sizes is likely mainly due to unresolved repetitive regions. BUSCO percentages for the final assemblies indicated a high level of completeness for both genomes (89.6% for *H. symbiolongicarpus* and 89.1% for *H. echinata*; Supplemental Table S3). Karyotype analysis of *H. symbiolongicarpus* previously reported 15 pairs of chromosomes (2n = 30) for this species (Chen et al. 2023), consistent with the chromosome count of several other cnidarians, including *H. vulgaris, C. hemisphaerica* (Munro et al. 2023) and *Nematostella vectensis* (Zacharias et al. 2004; Putnam et al. 2007; Guo et al. 2018).

Gene model prediction and annotation

Using RNA-seq reads and assembled transcripts from adult animals to guide the annotation process, we predicted genes for each genome using AUGUSTUS (Haas et al. 2008), with detailed methods provided in Supplemental Data S1 and S2 and summary statistics in Supplemental Table S3. 22,022 genes were predicted for *H. symbiolongicarpus* and 28,825 for

Downloaded from genome.cshlp.org on June 12, 2026 . Published by Cold Spring Harbor Laboratory Press

H. echinata. Coding regions make up about 8% of each assembly, while noncoding regions account for 92%. On average, *H. symbiolongicarpus* has 7.47 exons and 6.47 introns per gene, compared to 6.60 exons and 5.60 introns per gene in *H. echinata* (Supplemental Table S5). The average intergenic region is 6,679 bp for *H. symbiolongicarpus* and 7,603 bp for *H. echinata* (Supplemental Table S5). 5' and 3' UTR predictions were performed with PASA (Haas et al. 2008), indicating that 48% (*H. symbiolongicarpus*) and 42% (*H. echinata*) of the gene models have predicted UTRs. Some *Hydractinia* transcripts undergo trans-spliced leader addition processing that is known to occur in hydrozoan genomes (Stover and Steele 2001; Derelle et al. 2010). The replacement of 5' UTR sequences by short sequences that are trans-spliced from non-coding spliced leader RNAs occurs in a few distantly related animal groups, as well as in several unicellular eukaryotes (Hastings 2005). We detected spliced leader sequences in our mRNA sequencing data, as well as spliced leader genes. Our ability to accurately predict 5' UTRs for some gene models was likely impacted by this phenomenon.

We evaluated completeness of the predicted gene models via BUSCO v5 (*9*) with the Metazoa dataset of 954 proteins. For *H. symbiolongicarpus*, there were 92.5% complete and 10.2% duplicated genes (Supplemental Tables S3, S12 tab SM1), while there were 90.7% complete and 12.3% duplicated genes in *H. echinata* (Supplemental Tables S3, S12 tab SM1). The number of duplicated genes may be slightly elevated due to our gene prediction pipeline strategy (Supplemental Material). We determined the percentage of gene models that had assembled transcript support and performed functional annotation on these gene models, combining our RNA-seq data from adult animals with additional RNA-seq data from *H. symbiolongicarpus* developmental stages or *H. echinata* polyp head regeneration timepoints (Supplemental Material; Supplemental Code S1; Supplemental Tables S6, S7) for our transcript support analysis. Overall, 78% of *H. symbiolongicarpus* gene models and 63% of *H. echinata* gene models had transcript support with at least 90% gene overlap (Supplemental Figs. S2-S5;

Downloaded from genome.cshlp.org on June 12, 2026 . Published by Cold Spring Harbor Laboratory Press

Supplemental Table S8). A small percentage of gene models had no overlapping transcript support (14% *H. symbiolongicarpus*, 21.5% *H. echinata*; Supplemental Figs, S2, S4; Supplemental Table S8). Functional annotation of gene models was performed using several approaches that included a DIAMOND search (Buchfink et al. 2015) of NCBI's nr database and using PANNZER2 (Törönen et al. 2018) (Supplemental Material; Supplemental Table S9). Overall, 88.5% of *H. symbiolongicarpus* gene models and 76.2% of *H. echinata* gene models had some level of annotation: a DIAMOND hit to NCBI nr, a PANNZER2 hit, or both (Supplemental Table S9).

Mitochondrial Genome

Cnidarians are characterized by mitochondrial genomic diversity, varying in overall mtDNA conformation (circular or linear), gene content, gene organization, and the number of mitochondrial chromosomes within each species (Kayal et al. 2012; Smith et al. 2012; Kayal et al. 2015). Medusozoan cnidarians possess linear monomeric or multimeric mitochondrial chromosomes, while most anthozoan cnidarians possess circular mtDNA (Supplemental Fig. S6) (Kayal et al. 2012, 2015; Bridge et al. 1992; Brugler and France 2007). The typical mtDNA observed in cnidarians consists of a set of 17 genes: the small and large ribosomal genes, methionine and tryptophan transfer RNA genes, and 13 energy pathway proteins (Bridge et al. 1992; Beagley et al. 1998). These genes are usually organized in the same transcriptional orientation, with a partial or complete extra copy of the *Cox1* gene in the opposite transcriptional orientation at one end of the chromosome (Kayal and Lavrov 2008). Secondary structures in intergenic regions and at the ends of the mtDNA regions may be involved in the control of replication and transcription (Brugler and France 2007; Stampar et al. 2019) and are also thought to protect the ends of the mitochondrial chromosome given their lack of traditional telomeric repeats, as previously observed in *Hydra oligactis* (Kayal et al. 2012; Smith et al.

Downloaded from genome.cshlp.org on June 12, 2026 . Published by Cold Spring Harbor Laboratory Press

2012; Brugler and France 2007; Beagley et al. 1998). Furthermore, introns, duplicated genes, and several additional protein-coding genes have been observed in several non-hydrozoan cnidarian mitogenomes (Beagley et al. 1998; Shao et al. 2006; Chen et al. 2008; Voigt et al. 2008).

The linear mitochondrial genome of *Hydractinia* is located on a single scaffold in both *Hydractinia* species, containing the coding sequences for the large (*16S/RNL*) and small (*12S/RNS*) ribosomal subunits, mitochondrial transfer RNA (tRNA) genes, all cnidarian mitochondrial proteins (*Cox1-3*, *Cob*, *Nad1-6*, and *Nad4L*), and inverted terminal repeats (ITRs) that form G-rich loops at both ends of the molecule. This strongly suggests that *Hydractinia* contains only one mitochondrial chromosome, similar to what has been observed in other hydrozoan genomes (Supplemental Fig. S7, Supplemental Table S10) (Kayal et al. 2012; Smith et al. 2012; Kayal and Lavrov 2008). *Hydractinia*'s mitochondria are mostly devoid of tRNAs, with both species containing just one tRNA-Met sequence and one tRNA-Trp sequence (Supplemental Fig. S8). These sequences form the characteristic tRNA hairpin structure and are in non-coding regions (Supplemental Fig. S8). An alternative mechanism for the replication and expression of linear mitochondrial genomes has been suggested, where transcription and replication occur in two directions, starting from a large intergenic spacer (Kayal et al. 2015). The origin of replication (Ori) is characterized by stable stem-loop configurations containing T-rich loops and abrupt changes in DNA composition bias (Brugler and France 2007; Stampar et al. 2019). Based on these characteristics, we propose that the origin of replication in *Hydractinia* is in the intergenic spacer between the large ribosomal subunit (*16S/RNL*) and the *Cox2* gene (Supplemental Figs. S7, S9). The ITRs of both *Hydractinia* species can form G-rich loops that likely protect the ends of these linear mitochondrial chromosomes in the absence of telomeric sequences (Supplemental Fig. S10). In addition, the presence of non-functional (and gradually degrading) nuclear copies of mtDNA (NUMTs) have previously been identified in *H. vulgaris*

Downloaded from genome.cshlp.org on June 12, 2026 . Published by Cold Spring Harbor Laboratory Press

(Song et al. 2013). Sequence similarity searches did not detect NUMTs within either *Hydractinia* genome. This result was confirmed by the lack of sequence variance in Illumina raw reads mapped to their mitochondrial genomes. Other cnidarians with linear mtDNAs, such as the jellyfish *Sanderia malayensis* and *Rhopilema esculentum*, were also shown to not contain NUMTs (Nong et al. 2020).

Orthology inference, phylogenetic analyses, and divergence time estimates

Orthology inference analysis was performed on a splice-filtered dataset (Supplemental Data S3) consisting of proteomes from 49 eukaryotic species encompassing 15 animal phyla and four non-animal outgroups (Supplemental Material; Supplemental Table S11). Taxon selection was initially based on a data set used by Maxwell et al. (2014) to infer the evolutionary origins of human disease-associated gene families that was then expanded to place the *Hydractinia* genomes in an evolutionary context with other cnidarian genomes. To that end, 16 cnidarian species spread across the main cnidarian lineages were included. This represents the largest sampling of cnidarians in any genome-wide orthology inference study performed to date and provides increased resolution for characterizing evolutionary dynamics among cnidarians, as well as between cnidarians and other animals. An input species tree (Supplemental Fig. S11) based on the current literature was provided to OrthoFinder v2.2.7 (Emms and Kelly 2019). A total of 33,325 orthogroups containing 81.2% of the proteins were recovered in the dataset. These orthogroups were then used as the basis for the analyses described below (Supplemental Data S3-S9).

For our phylogenetic analysis, we selected a subset of single copy ortholog (SCO) sequences from our orthogroup data set (Supplemental Data S10). These SCOs were chosen for their presence in at least 12 of 15 cnidarian species; four bilaterian and three non-bilaterian outgroup

Downloaded from genome.cshlp.org on June 12, 2026 . Published by Cold Spring Harbor Laboratory Press

261 species that also contained these SCOs were included in the analysis. The final concatenated,
262 aligned, and trimmed data set included sequences from 216 orthogroups, resulting in an
263 alignment of 50,457 nucleotides (Supplemental Data S10). The resulting maximum likelihood
264 tree, generated using IQ-Tree2 (Supplemental Data S11), confirmed known relationships within
265 Cnidaria, including placing the two *Hydractinia* species closest to *C. hemisphaerica* (Fig. 1B).
266 This tree was then used to estimate divergence times within the phylum using r8s (Sanderson
267 2003). Our age estimate for the most recent common ancestor of anthozoans is 496.6 MYA,
268 while that of medusozoans is 538.9 MYA. While the estimated ages for clades within Cnidaria
269 tend to be older than those previously reported (Khalturin et al. 2019), we find that the
270 divergence time between the two *Hydractinia* species to be just 19.16 MYA (Fig. 1B). Providing
271 an alternative input species tree with Porifera at the base did not significantly alter overall
272 results of orthology inference or divergence time estimates (Supplemental Fig. S12).
273
274 **Synteny**
275
276 We performed pairwise macrosynteny analyses comparing *H. symbiolongicarpus* and *H.*
277 *echinata*, as well as a series of comparisons between each *Hydractinia* species and *C.*
278 *hemisphaerica*, *H. vulgaris*, and *N. vectensis* by clustering scaffolds of these species based on
279 the shared orthogroup numbers (Supplemental Material; Supplemental Code S1). Despite not
280 having chromosomal-level assemblies, we observed local collinearity between the two
281 *Hydractinia* species (Fig. 1C) and general chromosomal-level conservation beyond scaffold
282 boundaries, as evidenced by scaffold clustering within the *Hydractinia* genus and beyond (Fig.
283 1C). This indicates a high degree of synteny between the two *Hydractinia* species, an
284 observation that is not surprising due to their close phylogenetic relationship and relatively
285 recent divergence (Fig. 1B). The observation that this conservation is shared with at least three
286 other cnidarian species (Fig. 1C, Supplemental Fig. S13) suggests that *Hydractinia*

Downloaded from genome.cshlp.org on June 12, 2026 . Published by Cold Spring Harbor Laboratory Press

chromosomes show a similar degree of ancestrality (Simakov et al. 2022). Further chromosomal-level assembly and analysis will be required to validate this hypothesis and identify features unique to *Hydractinia*.

Characterization of genomic repeats, including transposable elements

According to our RepeatMasker *de novo* analysis, genomic repeats comprise 55% of the *H. echinata* genome and 50% of the *H. symbiolongicarpus* genome. These figures are slightly lower than the percentage of repetitive DNA found in *H. vulgaris* (57%) but higher than that found in both *C. hemisphaerica* (39%) and *N. vectensis* (25%) (Supplemental Table S12) (Chapman et al. 2010; Putnam et al. 2007; Leclère et al. 2019). The overall composition of repeat classes is similar between the two *Hydractinia* species (Fig. 1D; Supplemental Fig. S14; Supplemental Tables S13-S16). The largest proportion of repeats are unclassified in both genomes, accounting for around 60% of all repetitive elements; these unclassified repeats comprise 35% and 30% of the *H. echinata* and *H. symbiolongicarpus* genomes, respectively.

Beyond the unclassified repeats, DNA transposons comprise the most abundant class of transposable element, accounting for about 20% of all repetitive elements and 11% of each genome. This is similar to what has been observed in both *N. vectensis* and *H. vulgaris*, where DNA transposons are the most abundant class of transposable elements. Some differences between the two species in several DNA transposon superfamilies were noted (Supplemental Fig. S14). Long interspersed nuclear elements (LINEs) accounted for 7% of all repetitive elements and 4% of each genome. Other repetitive element classes have similar compositions in the two genomes, except for long terminal repeat (LTR) retrotransposons. Although LTR retrotransposons only accounted for a small fraction of the genome in both species, there are some significant differences in their family composition and evolution between the species

Downloaded from genome.cshlp.org on June 12, 2026 . Published by Cold Spring Harbor Laboratory Press

(Supplemental Fig. S14). The LTR retrotransposons accounted for 2.6% of all repetitive elements in *H. echinata* and 3% in *H. symbiolongicarpus*, representing 1.5% and 3% of these genomes, respectively. We performed a repeat landscape analysis (Supplemental Material) that suggests a highly similar evolutionary history of invasion of repetitive elements in the two species (Fig. 1E, Supplemental Code S1) with differences between the species illustrated in Supplemental Figs. S15-S16. One such example is a recent species-specific expansion (at ~10% nucleotide substitution) of LTR retrotransposons in *H. symbiolongicarpus* (Supplemental Fig. S16). This small expansion was mainly composed of members of the Gypsy family of LTRs. The two genomes also harbor different types of endogenous retroviruses (ERVs). Endogenous retrovirus group K genes (ERKVs) are only present in *H. echinata*, whereas endogenous retrovirus group L genes (ERVLs) are only present in *H. symbiolongicarpus*, suggesting two recent independent invasions of ERVs after the speciation event around 19 MYA (Supplemental Fig. S16).

Orthogroup lineage specificity and overall patterns of evolutionary novelty

Recent cnidarian genome sequencing projects (Khalturin et al. 2019; Leclère et al. 2019; Gold et al. 2019) have demonstrated the contribution of both taxon-restricted and shared ancestral gene families to cnidarian-specific cell types, such as those found in the medusa. To evaluate the contribution of such gene families to evolutionary novelty in *Hydractinia*, we identified lineage-specific subsets of orthogroups. Out of the 33,325 orthogroups inferred by OrthoFinder, roughly 26% are cnidarian-specific, 16% are medusozoan-specific, 8% are hydrozoan-specific, 6% are specific to *Hydractinia* + *Clytia*, and just under 5% are specific to the genus *Hydractinia*. In comparison, only 7% of orthogroups are specific to anthozoans. *H. echinata* possesses 46 species-specific orthogroups, while *H. symbiolongicarpus* possesses just 15 such orthogroups.

Downloaded from genome.cshlp.org on June 12, 2026 . Published by Cold Spring Harbor Laboratory Press

Additionally, based on our sampling of 23 bilaterian species from a variety of phyla, the percentage of bilaterian-specific orthogroups (~24%) is similar to the 26% found in cnidarians.

To evaluate the contribution of conserved gene families to *Hydractinia*'s evolution and further evaluate the broad suitability of cnidarians as animal models, we calculated the overlaps of orthogroups between major groups of cnidarians and bilaterians (Supplemental Fig. S17, Supplemental Data S13-S15). At the broadest scale, cnidarians and bilaterians possess more shared than unshared orthogroups. This supports previous observations based on the genome sequences of *Hydra* (Chapman et al. 2010) and *Nematostella* (Putnam et al. 2007) that much of the cnidarian toolkit predates the divergence of Cnidaria and Bilateria. Splitting Cnidaria further into the Medusozoa and Anthozoa (Supplemental Fig. S17A), we observe that the number of orthogroups unique to Medusozoa + Bilateria is nearly equal to that for Anthozoa + Bilateria, both of which are greater than the number for Medusozoa + Anthozoa. This is consistent with numerous observations of deep divergence between medusozoan and anthozoan genomes, from fossil estimates to divergence time estimates (Steele et al. 2011; Khalturin et al. 2019).

To further investigate potential sources of evolutionary novelty, we calculated the percentage of genes within each species that are assigned to orthogroups that are species-specific, the percentage of phylum-specific and metazoan-specific genes, and the percentage of genes unassigned to an orthogroup. These five proportions are visualized in the right panel of Fig. 2 for the 15 cnidarian species that were analyzed further using CAFÉ (see below). Proportions for all metazoan species in our analysis are visualized in Supplemental Fig. S18. The two *Hydractinia* species contain the highest percentages of phylum-specific genes of all 43 metazoan species we examined (23% and 22%, respectively), thereby indicating that their genomes contain the highest percentage of cnidarian-specific genes of all cnidarians included in this analysis. Coupled with the fact they possess relatively few species-specific orthogroups,

Downloaded from genome.cshlp.org on June 12, 2026 . Published by Cold Spring Harbor Laboratory Press

this suggests that a significant proportion of their proteomes may have evolved at the genus, family, or subphylum level, which are grouped together under 'Phylum-specific' in the analysis featured in Fig. 2. Additionally, a DIAMOND search indicated that most (90%) unassigned *Hydractinia* genes had no match in the NCBI nr database (Supplemental Table S11 tab X.4). Transcript support for these genes (Supplemental Table S8) indicates that a large proportion of these genes have >90% transcript overlap (51.28% in *H. symbiolongicarpus* and 35.35% in *H. echinata*) and are expressed by the animal. Thus, the two *Hydractinia* genomes appear to contain an abundance of evolutionarily novel genes.

Estimating the evolutionary dynamics of gene families using CAFÉ

Focusing just on the Cnidaria + Bilateria subtree (19 species) derived from the 22 species tree inferred using IQ-Tree2 and r8s (described above), we estimated the evolutionary dynamics of the 8,433 OrthoFinder-inferred orthogroups that are present in the ancestor of this subtree (Supplemental Material; Supplemental Data S16-S27). Using CAFE, gene family dynamics were estimated for each node and terminal taxon (De Bie et al. 2006; Han et al. 2013) in our subtree and are summarized as Fig. 2 (left panel), with additional details available in Supplemental Table S11, Tab X.8.

Across the whole tree (Fig. 2), more changes in gene family size take place on the terminal branches of the tree than in the internal branches of the tree. Terminal branches have significantly more gene expansion or contraction as compared to internal branches [mean(terminal) = 2,375.7, mean(internal) = 1007, t = 8.5139, df = 33.99, *p*-value = 6.07×10^{-10}]. This pattern is very clear when comparing the internal nodes of the cnidarian phylum with the terminal branches of this group (Fig. 2). Of the 8,433 analyzed orthogroups, a total of 592 were found to be evolving rapidly on the subtree (Viterbi *p*-value <= 0.05). The distribution of these

Downloaded from genome.cshlp.org on June 12, 2026 . Published by Cold Spring Harbor Laboratory Press

uniquely fast-evolving gene families per taxon/node can be found in Supplemental Table S11, Tab X.8, and information about their putative identities can be found in the Supplemental Material.

Comparing evolutionary dynamics of H. symbiolongicarpus and H. echinata using CAFE

Roughly half of the orthogroups present in the *Hydractinia* genomes and included in the CAFE analysis have undergone some change in size (50% in *H. symbiolongicarpus* and 54% in *H. echinata*) when comparing their observed size to the inferred size of these orthogroups in the Cnidarian+Bilaterian ancestor. Notably, the two *Hydractinia* genomes have very different proportions of gains versus losses over their terminal branches. *H. echinata* has experienced more expansions with a higher number of genes per expansion, resulting in *H. echinata* gaining about twice as many (1.97×) individual gene copies in the past 19 million years. Conversely, *H. symbiolongicarpus* has a higher number of contracted gene families and has lost more genes per contraction, meaning that *H. symbiolongicarpus* has lost nearly 2.5 times more genes in total than *H. echinata* has since their divergence. Additionally, although *H. echinata* and *H. symbiolongicarpus* have lost 248 and 252 gene families, respectively, the identities of the lost families do not overlap at all. This implies that these species have undergone very different evolutionary trajectories since their divergence roughly 19 MYA. We performed additional comparisons of evolutionary dynamics in *Hydractinia* versus the other hydrozoan taxa (*H. vulgaris* and *C. hemisphaerica*) and versus the genus *Aurelia* (Supplemental Material). Overall, *H. vulgaris* and *C. hemisphaerica* have more taxon-specific orthogroup size changes than either species of *Hydractinia*. However, when combining data from the two *Hydractinia* species to look at changes at the genus level, the number of changes are roughly similar between these hydrozoans. For the comparison with *Aurelia*, we found that the overall proportions of gains

Downloaded from genome.cshlp.org on June 12, 2026 . Published by Cold Spring Harbor Laboratory Press

versus losses was much more similar between the two *Aurelia* lineages, in contrast with what we found for the two *Hydractinia* species (Supplemental Material; Supplemental Fig. S19).

The non-coding RNA landscape: miRNAs

microRNAs (miRNAs) constitute a unique class of small non-coding RNAs of approximately 22 nucleotides (nt) in size that play crucial roles in development, cellular differentiation, and stress response in both plants and animals (Wheeler et al. 2009). Several studies have investigated miRNAs and the miRNA pathway in cnidarians (Moran et al. 2013; Praher et al. 2021). We generated small RNA-seq libraries for five samples of adult *H. echinata* polyps that were then sequenced (Supplemental Material). The resulting reads were trimmed and mapped to the *H. echinata* genome using the miRDeep2 mapping algorithm (Friedländer et al. 2012), yielding 347 predicted miRNAs. Subsequent custom automated filtering and manual screening of this set of miRNAs was performed to identify the highest quality predicted miRNAs from this set, producing a final list of 38 unique high-quality mature miRNA sequences (Supplemental Figs. S20, S21; Supplemental Table S17). Of these, three are homologous to known cnidarian miRNAs (miR-2022, miR-2025, and miR-2030), with alignments shown in Supplemental Fig. S22. Supplemental Fig. S23 depicts a proposed evolutionary scenario for miRNAs in cnidarians that includes these new data from *H. echinata*.

The non-coding RNA landscape: rRNAs, tRNAs, and snoRNAs

In an attempt to provide the first detailed description of the non-coding RNA (ncRNA) landscape of any cnidarian species, we found that the two *Hydractinia* genomes encode the expected suite of functional non-coding RNAs commonly present in metazoan genomes. These included ribosomal RNA genes (rRNAs), transfer RNAs (tRNAs) for each amino acid isotype,

Downloaded from genome.cshlp.org on June 12, 2026 . Published by Cold Spring Harbor Laboratory Press

spliceosomal RNAs for both the major (U1, U2, U4, U5 and U6) and minor spliceosome (U11, U12, U4atac, and U6atac), small nucleolar RNas (snoRNAs), SRP RNA, RNase P RNA, RNase MRP RNA, and Vault RNA (Supplemental Table S18). This characterization was based on results from Rfam (Kalvari et al. 2018), Infernal (Nawrocki and Eddy 2013), and tRNAscan-SE (Chan et al. 2021) (Supplemental Material). An unusual feature of many of these ncRNAs is their apparent organization into roughly evenly spaced tandem arrays of tens or even hundreds of nearly identical or highly similar copies. Each of these copies is separated by spacer regions ranging in length from several hundred to a few thousand nucleotides that are nearly identical or highly similar to one another (Supplemental Tables S19-S21; Supplemental Data S28-S36). In both *Hydractinia* genomes, these arrays include ribosomal RNAs, four of the five RNA components of the major spliceosome (U1, U2, U5, and U6), the small nucleolar RNA U3, and tRNAs for each of the 20 amino acids (Supplemental Tables S18 S21-25). Although tandem arrays of some RNA genes – especially clusters of ribosomal RNA genes collectively known as rDNA – are common in eukaryotes (Cloix et al. 2000; Long and Dawid 1980), tandem array organization of tRNAs (Bermudez-Santana et al. 2010) is unusual outside of the *Entamoeba* genus of *Amoebozoa* (Tawari et al. 2008), with only one such example having been observed in mammals (Darrow and Chadwick 2014). The ncRNA tandem arrays only make up a small percentage of all regions that appear in tandem repeats in the *Hydractinia* assemblies. Tandem repeat regions detected using TRF (Benson 1999) having seven or more copies with a period length of 50 nt and ≥75% average similarity between repeats cover 18.7% of the *H. echinata* and 15.7% of the *H. symbiolongicarpus* assemblies. These TRF-defined repeats are largely a subset of the unclassified repeats identified by our RepeatMasker analysis detailed above (88.1% of the *H. echinata* and 72.0% of the *H. symbiolongicarpus* nucleotides in the TRF-defined repeat regions also exist in the unclassified repeat regions). The nucleotides covered by the RNA tandem arrays account for only 4.8% and 7.7% of these TRF-defined repetitive regions in *H. echinata* and *H. symbiolongicarpus*, respectively. While the biological significance of these

Downloaded from genome.cshlp.org on June 12, 2026 . Published by Cold Spring Harbor Laboratory Press

ncRNA tandem arrays and other tandem repeat regions remains unclear in the absence of functional data, two important observations argue against the presence of these RNA tandem arrays being due to sequencing or assembly artifacts. First, when comparing these results to other cnidarian species, we were able to identify tandem arrays of 5S rRNA, tRNA, and U5 RNA in the *N. vectensis* genome (Putnam et al. 2007) but did not find RNA tandem arrays in other cnidarian genomes. Secondly, the draft genome assembly of *H. echinata*, sequenced and assembled using different methods (Török et al. 2016) than the primary *H. echinata* assembly presented here, also includes tandem arrays of 5S rRNA, SRP RNA, and tRNA and a significant fraction of that assembly is also in TRF-defined tandem repeats (5.1% of the genome).

The homeobox gene complement of *Hydractinia*

Homeobox genes are a large superfamily of protein-coding genes that encode for a 60 amino acid helix-turn-helix domain called the homeodomain (Holland 2013). Most homeobox genes are DNA-binding transcription factors (Holland 2013) that play key roles in early embryogenesis (Driever and Nüsslein-Volhard 1988), patterning (Pearson et al. 2005), development of the nervous system and sensory organs (Schulte and Frank 2014), and maintenance of embryonic stem cells (Young 2011). We identified 71 homeodomain-containing genes in the *H. symbiolongicarpus* genome and 82 in the *H. echinata* genome. Phylogenetic (Supplemental Figs. S24, S25; Supplemental Data S37-S42) and secondary domain architecture-based approaches were able to resolve the ANTP, CERS, LIM, POU, PRD, SINE, and TALE homeobox classes, with a small number of genes remaining unclassified (Supplemental Table S26). In both species, the ANTP-class homeodomains were the most abundant. Overall, *H. echinata* has 11 more homeobox genes than *H. symbiolongicarpus*, with expansions in the CERS, LIM, POU and PRD classes (Supplemental Table S26). Four unclassified homeobox genes are unique to *H. echinata*. It is possible that some of these expansions in *H. echinata*

Downloaded from genome.cshlp.org on June 12, 2026 . Published by Cold Spring Harbor Laboratory Press

493 may be duplicates from different alleles of the same gene that were not properly phased during
494 the separation of haplotypes during the assembly process. All seven unclassified genes in *H.*
495 *symbiolongicarpus* have a homolog to an unclassified gene in *H. echinata* (Supplemental Table
496 S27). Class-based annotation of homeodomain-containing genes based on phylogenetics,
497 secondary domain information, and associated results from OrthoFinder for both *Hydractinia*
498 species can be found in Supplemental Table S27.
499
500 **The HOX-L subclass of homeodomains in *Hydractinia***
501
502 Some of the most interesting genes to evolutionary biologists are those belonging to the Hox
503 families of homeobox genes (Procino 2016). Hox genes are members of the ANTP class of
504 homeoboxes, along with the Hox-like ('extended Hox') genes *Eve*, *Meox/Mox*, *Mnx,* and *Gbx*;
505 the ParaHox cluster of *Gsx*, *Cdx*, and *Pdx/Xlox*; and the NK-like gene subclass (Holland 2013;
506 Holland et al. 2007). The ANTP class is the largest and most diverse class, consisting of over
507 50 families; 37 of these families containing over 100 genes have been identified in humans
508 (Holland et al. 2007). Hox and ParaHox genes are thought to have emerged prior to animal
509 evolution and were subsequently lost, reduced, or absent in early-emerging taxa (Mendivil
510 Ramos et al. 2012; Steinworth et al. 2023). In many bilaterians, Hox genes are arranged in at
511 least one chromosomal cluster (Duboule 2007). Genomic linkage between Hox genes is present
512 in extant cnidarians, although linked Hox and ParaHox genes were not found in previous
513 cnidarian genome studies (Chapman et al. 2010; Putnam et al. 2007; Khalturin et al. 2019;
514 Leclère et al. 2019; Gold et al. 2019; Jeon et al. 2019; DuBuc et al. 2012).
515
516 Both *Hydractinia* species possess several genes that belong to the HOX-L subclass
517 (Supplemental Figs. S26, S27; Supplemental Data S43-S48). These include several non-
518 anterior (CenPost) cnidarian Hox genes, the ParaHox genes *Gsx* and *Cdx*, and the Hox-

Downloaded from genome.cshlp.org on June 12, 2026 . Published by Cold Spring Harbor Laboratory Press

519 extended group *Mox*. The anterior Hox genes *HoxA1* and *Hox2/Gsx-like* genes are absent in
520 both species even though these genes have been found in other cnidarians, including
521 hydrozoans (Chiori et al. 2009; Ryan et al. 2006). Additional members of the HOX-L repertoire
522 that are present in other cnidarians but are absent in *Hydractinia* are genes encoding for the
523 Hox-extended gene *Eve* and the ParaHox genes *Pdx/Xlox* (Leclère et al. 2019; Gold et al. 2019;
524 Ryan et al. 2006) (Fig. 3). A primitive Hox cluster has been observed in anthozoan cnidarians
525 but has not been found in hydrozoans (Chourrout et al. 2006; DuBuc et al. 2012). However,
526 there appears to be some linkage of Hox genes in both *Hydractinia* genomes (Fig. 3). This
527 includes linkage of several cnidarian specific Hox genes in *H. symbiolongicarpus* and linkage of
528 a cnidarian Hox gene with the ParaHox gene *Gsx* in both *Hydractinia* species. Prior to this
529 study, the linkage of a Hox and ParaHox gene has not been shown in any other cnidarian
530 genome. A comparison of phylogenetic relatedness and synteny analysis of various cnidarian
531 species suggests that *Hydractinia* species likely lost the HOX-L genes *HoxA1* and *Eve* (Fig. 3).
532 These genes are clustered together in anthozoans (DuBuc et al. 2012; Zimmermann et al.
533 2023) and *Eve* is found in close proximity to human Hox clusters (Faiella et al. 1991; D'Esposito
534 et al. 1991). In contrast, *Hydra* has retained a *HoxA1* homolog but has also lost *Eve* (Chapman
535 et al. 2010).
536
537 To determine the spatial patterning role of some of the homeobox genes relative to other known
538 expression patterns, we performed colorimetric RNA *in situ* hybridization. Expression patterns
539 for a subset of Hox genes at different stages of *Hydractinia*'s life cycle were determined
540 (Supplemental Fig. S28). Overall, several genes show a somatic patterning role during early
541 larval formation, while other Hox genes are maternally expressed during sexual development.
542 This suggests that Hox genes may have an important role in egg formation.
543

Downloaded from genome.cshlp.org on June 12, 2026 . Published by Cold Spring Harbor Laboratory Press

The Allorecognition Complex

Allorecognition is controlled by at least two linked genes, *Allorecognition 1* (*Alr1*) and *Allorecognition 2* (*Alr2*) in *Hydractinia* (Nicotra 2019; Nicotra et al. 2009; Rosa et al. 2010). Both encode single-pass transmembrane proteins with highly polymorphic extracellular domains, with the allorecognition response being controlled by whether colonies share alleles at these loci. In previous work, we examined the partially assembled genome of a strain of *H. symbiolongicarpus* that is homozygous at *Alr1* and *Alr2* and discovered that both genes are part of a family of immunoglobulin superfamily genes that reside in a genomic interval called the allorecognition complex (ARC) (Huene et al. 2022). We identified *Alr1* and *Alr2* on separate scaffolds within the *H. symbiolongicarpus* reference genome, as well as a second *Alr1* allele on a third scaffold. These alleles were likely retained in the final assembly because they were sufficiently divergent from each other not to be recognized as alleles of the same gene. We identified 19 additional genes predicted to encode full-length Alr proteins similar to those previously described (Huene et al. 2022), as well as 44 gene models with some sequence similarity to Alr1 or Alr2 that were not predicted to encode cell surface proteins, suggesting they were pseudogenes. Within the reference genome, most of these Alr1/Alr2-like gene models are located in four clusters (Supplemental Fig. S29). Additional work will be required to phase these contigs into two ARC haplotypes and assign orthology between them and the Alr genes already identified (Huene et al. 2022). The Huene et al. (2022) study found that there are at least 41 *Alr*--like loci in this region, with more than half of these genes located within one of three Alr clusters. While the individual Alr proteins encoded by these genes have low overall sequence identity, the domain architecture of these proteins, along with structure-based predictions using AlphaFold, confirm that these Alr proteins are members of the immunoglobulin superfamily (Huene et al. 2022).

Downloaded from genome.cshlp.org on June 12, 2026 . Published by Cold Spring Harbor Laboratory Press

Single-cell transcriptomics of adult animals

A critical part of establishing *Hydractinia* as a useful research organism is having a list of cell-type specific markers for all cell types in the adult animal. Single cell transcriptome analysis of adult *H. symbiolongicarpus* 291-10 male animals was performed using the 10x Genomics platform (Supplemental Material). Briefly, cell suspensions of dissociated adult feeding and sexual polyps and associated connective mat tissue were prepared and two samples were resuspended in different final buffers (3XPBS or calcium- and magnesium-free seawater minus EGTA) followed by subsequent 10x single-cell library construction. These two libraries were then sequenced using the Illumina NovaSeq 6000 sequencing system. Statistics from each library can be found in Supplemental Table S28. The two libraries were ultimately combined after analyzing them separately (Supplemental Fig. S30) and determining that they were very similar. Downstream analyses of these sequence data were performed with both the 10x Cell Ranger pipeline version 7.0.1 and the Seurat version 4.3.0 (Satija et al. 2015), ultimately yielding heatmaps and UMAP plots for the visualization of cell clusters (Supplemental Material; Supplemental Data S49). The final clustering after filtering of technical artifacts (primarily removing sperm captured with another cell, termed ‘sperm doublets’; see Supplemental Material; Supplemental Data S49) with Seurat resulted in 18 clusters from a total of 8,888 cells (Fig. 4A). A heatmap was generated to show top variable ‘marker’ genes for each cluster (Supplemental Fig. S31).

Each cluster was then classified as a putative cell type or cell state through the annotation of these marker genes; these included distinct clusters of ectodermal (epidermal) and endodermal (gastrodermal) epithelial cells, mucous and zymogen gland cells, neurons, nematoblasts, nematocytes, germ cells, developing stages of sperm, and two clusters of i-cells (Fig. 4A). These i-cell clusters probably include early progenitor cells as pluripotent i-cells are a rare

Downloaded from genome.cshlp.org on June 12, 2026 . Published by Cold Spring Harbor Laboratory Press

596 population (Varley et al. 2023; Chrysostomou et al. 2022; DuBuc et al. 2020), thus we have
597 labeled them as ISC/prog on our UMAP. UMAP expression patterns for individual genes that
598 were used to identify and annotate the clusters based on previous literature can be found in
599 Supplemental Fig. S32 and further details are provided in Supplemental Table S29. We grouped
600 these clusters into seven major cell 'types': Sperm and Spermatocytes (clusters C0, C1, and
601 C4), Nematocytes (C2, C5, C8, and C9), Epithelial Cells (C3, C13, and C14), i-cells/Germ Cells
602 (C6 and C7), Nematoblasts (C10, C12, and C16), Neurons (C11), and Gland Cells (C15 and
603 C17).
604
605 A subset of seven different cell-type marker genes were chosen for fluorescence *in situ*
606 hybridization (FISH) for validation and to visualize spatial expression patterns of various cell
607 types in adult polyps (Fig. 4B-H), including two genes that have been previously published for
608 *Hydractinia* [*Piwi1* for marking i-cells/progenitors and *Ncol1* for marking all stages of maturing
609 nematoblasts (Bradshaw et al. 2015)]. The five remaining genes can be considered new cell-
610 type markers for *Hydractinia*. We observed that the proliferating cell nuclear antigen *PCNA*, a
611 known proliferation and broad stem cell marker in other animals (Wagner et al. 2011), marks
612 cells present in the i-cell band; *SLC9C1*, a member of the sodium-hydrogen exchanger (NHE)
613 family required for male fertility and sperm motility (Wang et al. 2003) marks mature sperm in
614 gonads of male sexual polyps; *nematocilin A*, a known structural component of the cnidocil
615 mechanosensory cilium trigger of mature cnidocytes in *Hydra* (Hwang et al. 2008), marks
616 mature cnidocytes in tentacles; *ARSTNd2-like* (previously undescribed) marks cnidocytes in the
617 polyp body column, and *Chitinase1*, a gland/secretory cell marker in cnidarians (Klug et al.
618 1984; Sebé-Pedrós et al. 2018) marks endodermal gland cells. These results represent a
619 significant step towards defining the major cell types in *Hydractinia* and the gene expression
620 patterns that define them. A list of all cluster marker genes according to cell type from the
621 Seurat analysis can be found in Supplemental Table S30.

Downloaded from genome.cshlp.org on June 12, 2026 . Published by Cold Spring Harbor Laboratory Press

We then explored the evolutionary profile of marker genes from the 18 individual clusters and the seven cell types (split further into nine groups; Fig. 5A) using strict filtering criteria (Supplemental Material). We found that, compared with other cell types (and clusters), i-cells and progenitors (ISC/prog cluster 6, 5.3% lineage-specific; ISC/germ cluster 7, 12.5% lineage-specific; all i-cells and progenitors, 9.5% lineage-specific) and early spermatogonia (cluster 4, 9.7% lineage-specific) are defined primarily by genes that are shared with other animals rather than lineage-specific genes, providing evidence that the toolkit employed by these cell types has a shared ancestry with other animals (Fig. 5A). Nematoblasts and nematocytes – cell types that are specific to cnidarians – were marked by a high proportion of phylum-specific or within-phylum genes (nematoblasts 49%, nematocytes 32.5%). Further probing into the i-cell cluster profile (clusters C6 and 7) to analyze how widespread the i-cell/progenitor marker genes were among animals in our dataset, we plotted how many species in our orthology-inference analysis shared each i-cell marker gene and found that the vast majority of the genes that mark i-cells are present in 40 or more species (Fig. 5B). Overall, our finding that the 317 i-cell marker genes were widely shared among all animals stands in contrast to the fact that the *H. symbiolongicarpus* genome has a higher proportion of phylum-specific and within-Cnidaria-specific genes (23%) than any of the other 41 animals in our orthology-inference analysis. The *Hydractinia* single cell dataset has an even higher proportion of phylum-specific and within-Cnidaria-specific genes (30.8%).

DISCUSSION

The extensive analyses performed in the course of this study have served to place the *Hydractinia* genome into a wider evolutionary context. In addition to providing an in-depth characterization of its nuclear genome, we determined that *Hydractinia* contains a single

Downloaded from genome.cshlp.org on June 12, 2026 . Published by Cold Spring Harbor Laboratory Press

mitochondrial chromosome. This is similar to what has been observed in other cnidarian species but differs from what has been observed in *Hydra*, which contains two mitochondrial chromosomes. Another significant difference observed between the genomes of these two species is that, while they are present in *Hydra*, we find no evidence for the presence of NUMTs in *Hydractinia*. A possible scenario giving rise to this difference may lie in the mechanism that severed the *Hydra* mitochondrial genome in two (see Supplemental Fig. S7 for the break region), enabling the introduction of mitochondrial sequences into the nuclear genome.

Our orthology analyses, which were based on both the predicted proteomes of the two *Hydractinia* species as well as the proteomes from 41 additional animal species and six related eukaryotes, provided a strong foundation for the subsequent analyses described here. The phylogenic analyses, which were based on conserved single-copy genes from species for which high-quality genomes are available, agreed with previous placements of *Hydractinia* within the hydrozoan cnidarians, positioning *Hydractinia* together with the hydrozoans *Clytia hemisphaerica* and *Hydra vulgaris*. While there are many additional hydrozoan taxa that have been placed between *Hydractinia* and *Clytia* based on various criteria, these species were not included in the present study due to a lack of available whole-genome sequence data. A sister taxon to *Hydractinia* is *Podocoryna,* whose genome is currently being sequenced; availability of these new genomic data will ultimately allow for more informative comparisons between these closely related groups. Comparing the two *Hydractinia* species to one another, divergence time analyses yielded an estimate that the two species diverged approximately 16 MYA. This estimate is much shorter than the estimated divergence times between lineages of the moon jelly *Aurelia aurita* [45.35 MYA in our study; 51-193 MYA reported by Khalturin et al. (2019)] and is more comparable to the divergence time between lineages of *Hydra vulgaris* [10-16 MYA; (Wong et al., 2019)].

Downloaded from genome.cshlp.org on June 12, 2026 . Published by Cold Spring Harbor Laboratory Press

Gene synteny analyses between the two *Hydractinia* species indicate a high degree of synteny which also extended to at least three other cnidarian species. We anticipate that macrosynteny analysis will only improve in the future with the increased availability of chromosomal-level cnidarian genome assemblies (Kon-Nanjo et al., 2023; Zimmerman et al., 2023). The repeat content analyses presented here indicate that at least 50% of each *Hydractinia* genome is comprised of repeats. Further, the overall repeat landscape was similar in the two species, with DNA transposons comprising the most abundant class of transposable elements, a finding similar to what has been observed in other cnidarian genomes (Putnam et al. 2007, Chapman et al. 2010).

Our orthology analyses indicate that 26% of the inferred orthogroups were cnidarian-specific, compared to the 24% of bilaterian-specific orthogroups from all sampled bilaterian species. This observation strongly suggests that the evolutionary novelty of orthogroups found across *all* of the Bilateria is equal to that found just within Cnidaria itself. Additional analyses focused on gene lineage specificity indicated that the two *Hydractinia* genomes possess the highest number of cnidarian-specific genes (22-23%) when compared to the other 15 cnidarian genomes that were included in the analysis. In addition, the vast majority of *Hydractinia* genes that did not ultimately cluster into any orthogroup also had no matches in GenBank, indicating that *Hydractinia* genomes contain a significant proportion of evolutionarily novel genes, well-positioning these genomes for subsequent studies of both novel and conserved genes. While these findings are obviously focused on evolution from a sequence-based perspective, future studies based on protein structure predictions and subsequent structure-based comparisons similar to those previously described for the freshwater sponge *Spongilla* (Ruperti et al., 2023) could further inform the degree of gene novelty within the *Hydractinia* genomes described here.

Downloaded from genome.cshlp.org on June 12, 2026 . Published by Cold Spring Harbor Laboratory Press

An evolutionary feature characterized in the course of this work involves the non-coding RNA (ncRNA) landscape of *Hydractinia*, the first such analysis in any cnidarian species. We were able to identify all of the functional ncRNAs that are also present in other animal genomes; these ncRNAs are organized into a large number of nearly identical or highly similar tandem arrays. Further, we could identify tandem arrays of 5S rRNA, tRNA, and U5 RNA in the *Nematostella* genome but not in any other published cnidarian genome, opening up an avenue for further study as more highly contiguous genome sequence data becomes available.

Given the importance and high degree of evolutionary conservation of homeodomain proteins, we have deduced the presence and absence of homeodomain-containing genes in the two *Hydractinia* species, using a phylogenetic approach to resolve the ANTP, CERS, LIM, POU, PRD, SINE, and TALE homeobox classes. Our analyses have provided evidence for the linkage of several cnidarian specific Hox genes in *H. symbiolongicarpus* and linkage of a cnidarian Hox gene with the ParaHox gene *Gsx* in both *Hydractinia* species. This has not been observed in any other cnidarian genome to date, providing evidence for the first time that bilaterian-like ParaHox genes may have once been located near the central/posterior region of the Hox cluster (Fig. 3). Further, this suggests that the last common ancestor of the cnidarians presumably had a linked Hox/ParaHox cluster flanked by NK-class and other homeobox genes (Fig. 3; D'Esposito et al. 1991). This finding could highlight that the breaking apart of the Hox and ParaHox cluster that occurred in the bilaterian ancestor may have been instrumental for their evolution.

Our characterization and analyses of *Hydractinia*'s allorecognition complex reinforce previous findings that Alr genes (and pseudogenes) are organized into a few discrete clusters covering a single large genomic region (Huene et al. 2022). The recent availability of chromosome-length genome sequence for *Hydractinia* (Kon-Nanjo et al. 2023), coupled with the highly annotated

Downloaded from genome.cshlp.org on June 12, 2026 . Published by Cold Spring Harbor Laboratory Press

data presented in this manuscript and methodological advances on the protein structure prediction front, is forming the foundation for future studies focused on the conservation of synteny within this gene complex across cnidarian species, studies that will, in turn, advance our understanding of the evolution of the immune system in bilaterians.

Through the use of single-cell transcriptomic approaches, we have created a robust cell-type atlas with well-annotated clusters which, in turn, has allowed us to identify specific genes that define individual cell types in adult animals. We identified two clusters with i-cell signatures which we designated ‘i-cells/prog’ which are cells heading toward a somatic fate and ‘i-cells/germ’ which are heading toward a germline fate. We observed some continuity between somatic i-cells and nematoblasts, as well as between somatic i-cells and neurons. We also found continuity between germline i-cells and cells involved in spermatogenesis in *Hydractinia*. This continuity was also observed in single-cell data from other hydrozoans such as *Hydra* (Siebert et al. 2019), where cells are continuously replaced and, to a lesser extent, in *Clytia* (Chari et al. 2021). We were not able to capture other cell state transitions (e.g., somatic i-cells to gland cells, or somatic i-cells to epithelial cells), as those clusters were isolated in the atlas. This likely reflects both the technical limitations of our sampling (8,888 cells in our atlas) and the biology of *Hydractinia*; turnover of these cell types is likely relatively low in adults as compared to *Hydra*, which has constant cell turnover in adult animals (Siebert et al. 2019). Further exploration of our cell type marker lists revealed that i-cells and progenitors are defined by genes that are highly conserved among animals, in contrast to most other cell types that contain a significant proportion of cnidarian-specific genes. This finding strongly suggests that there is a shared ancestry with other animals in the form of a conserved toolkit for regeneration. While it remains to be seen whether other animals do indeed share the same or partially overlapping toolkits of genes specifically within their stem cells – an important question that is beginning to be addressed using new methodologies currently under development (Wang et al. 2021) – the

Downloaded from genome.cshlp.org on June 12, 2026 . Published by Cold Spring Harbor Laboratory Press

results of the current study hold promise for future exploration from an evolutionary standpoint and, through a longer lens, potentially from a biomedical standpoint as well.

METHODS

Genome sequencing and assembly

Genomic DNA was prepared from adult polyps from a single strain for each species (291-10 males for *H. symbiolongicarpus* and F4 females from *H. echinata*). PacBio long-read and Illumina short-read data were generated. Canu was used as the contig assembler. Scaffolding was done by Dovetail HiRise scaffolding with Illumina Chicago libraries.

Gene model prediction and annotation

Gene models were generated with a pipeline that involved both PASA and AUGUSTUS. Strand-specific RNA-seq data from each species was used as input at different points of the pipeline as reads and as assembled transcripts. Functional annotation was performed with a DIAMOND search of NCBI's nr database and PANNZER2.

Orthology inference, phylogenetic analyses, and divergence time estimates

Orthology-inference analysis was performed on a splice-filtered proteome dataset of 49 species from 15 metazoan phyla and four non-metazoan outgroups. Orthology assignment was performed using OrthoFinder version 2.2.7 (Emms and Kelly 2019). Divergence times between *H. echinata* and *H. symbiolongicarpus* and between other cnidarian lineages were estimated by inferring a time-calibrated maximum-likelihood phylogeny using only single copy orthologs. The topology of our maximum likelihood phylogenetic tree was inferred using IQ-Tree2, and divergence date estimates were calculated for major nodes on the tree using a Langley-Fitch approach together with the TN algorithm, using r8s version 1.8.1 (Fig. 1B).

Downloaded from genome.cshlp.org on June 12, 2026 . Published by Cold Spring Harbor Laboratory Press

777

778 **Orthogroup lineage specificity and overall patterns**

779 Output from OrthoFinder was processed using custom R scripts (R Core Team 2021;
780 Supplemental Data S13-S15) to analyze patterns of presence and absence of orthogroups
781 across taxa and characterize the taxon-specificity of each orthogroup. Taxon specificity and
782 other related information for each *H. symbiolongicarpus* and *H. echinata* gene model can be
783 found in Supplemental Table S11 tabs 'X.10' and 'X.11'.

784

785 **Estimating the evolutionary dynamics of gene families using CAFE**

786 We used the software package CAFE v. 4.2.1 to estimate ancestral gene family sizes and
787 changes in gene family size among 15 cnidarian species, as well as to infer which gene families
788 are significantly faster evolving in specific cnidarian lineages. As input, we provided our time-
789 calibrated tree and the gene counts per species for a subset of the orthogroups inferred by
790 OrthoFinder.

791

792 **Single-cell transcriptomics of adult animals and OrthoMarker analyses**

793 Tissue from adult male *H. symbiolongicarpus* clone 291-10 was dissociated in 1% Pronase E in
794 calcium- and magnesium-free artificial seawater (CMFASW) with EGTA for 90 minutes total.
795 The cell suspension was filtered through a 70µm Flowmi cell filter, pelleted at 300 rcf for 5
796 minutes at 4C, and the pellet gently resuspended in either CMFASW without EGTA or 3 × PBS.
797 This cell suspension was filtered through a 40µm Flowmi cell filter and placed on ice. 10x single
798 cell 3' version 3 RNA-seq library construction was performed at the University of Florida's
799 Interdisciplinary Center for Biotechnology Research. Libraries were sequenced at the NIH
800 Intramural Sequencing Center using the Illumina NovaSeq 6000_SP sequencing system. The
801 10x Cell Ranger pipeline version 7.0.1 was used to pre-process the sequencing data for
802 downstream analysis. Seurat version 4.3.0 was used to generate clusters, find marker genes for

Downloaded from genome.cshlp.org on June 12, 2026 . Published by Cold Spring Harbor Laboratory Press

each cluster, and further analyze the data. A marker gene list for each cluster was created using Seurat and the settings used in Siebert et al. 2019. The OrthoFinder results (Supplemental Data S3-S9) were used to apply several levels of taxon-specificity to the marker gene list using R and the 'dyplr' package. The R package 'ggplot' was used to create the bar plot and histogram shown as Fig. 5a, 5b, respectively. Markers were validated with fluorescence *in situ* hybridization (Supplemental Material) and primers for those genes are found in Supplemental Table S31.

Data sets

All sequencing read data related to this project can be found in the SRA under BioProject PRJNA807936 (*H. symbiolongicarpus*) and PRJNA812777 (*H. echinata*).

Data access

The newly generated data from this Whole Genome Shotgun project has been deposited at DDBJ/ENA/GenBank under the accession JARYZW000000000 (*H. symbiolongicarpus*) and JASGCC000000000 (*H. echinata*). The version described in this paper is version JARYZW010000000 (*H. symbiolongicarpus*) and JASGCC010000000 (*H. echinata*). PacBio reads can be found in the SRA at SRX1436530, SRX14365302, SRX14365308, SRX14365309, and SRX14365310 (*H. echinata*) and SRX14210182, SRX14210183, and SRX14210193 (*H. symbiolongicarpus*). All Dovetail Chicago library sequencing data and mapping data for scaffolding assemblies, as well as additional data available for download, can be found at https://research.nhgri.nih.gov/hydractinia/download/index.cgi?dl=sd. All custom scripts are available in Supplemental Code S1. The *Hydractinia* Genome Project portal (https://research.nhgri.nih.gov/hydractinia) provides a rich source of data for both species,

Downloaded from genome.cshlp.org on June 12, 2026 . Published by Cold Spring Harbor Laboratory Press

including a BLAST interface, genome browser, DNA and protein sequence downloads, and functional annotation of gene models, as well as a single cell browser and RNA-seq expression data.

Competing interest statement

The authors declare no competing financial interests.

Acknowledgments

We would like to thank the following people: J. Spencer Johnston of Texas A&M University for propidium iodine-based genome size estimation. Rob Steele for providing *Hydra vulgaris* strain 105. Alice Young and many others at the NIH Intramural Sequencing Center (NISC) for DNA and RNA sequencing library construction, sequencing, as well as advice and support. Dovetail Genomics for providing Chicago libraries and scaffolding services. Leo Buss for advice and support. Gunter Plickert and Philipp Schiffer for early RNA-seq datasets not included in the final paper. Bernie Koch, Steve Bond, and Derek Gildea for advice and help. Suiyuan Zhang for making data available on the *Hydractinia* genome portal. Alexandrea Duscher for creating the *Chit1* riboprobe and assisting with the single-cell experiment. Mackenzie Simon-Collins for helping to optimize the cell dissociation protocol. Malcolm Maden for providing bench space during our single-cell experiment. Yanping Zhang and Alex Deiulio at the UF ICBR Gene Expression & Genotyping Core (RRID:SCR_019145) for advice and for constructing the 10x single-cell libraries. This work utilized the Biowulf high-performance supercomputing resource of the Center for Information Technology at the National Institutes of Health (https://hpc.nih.gov). This research was supported by the Intramural Research Programs of the National Human Genome Research Institute (ZIA HG000140 to A.D.B.) and National Library of Medicine (ZIB

Downloaded from genome.cshlp.org on June 12, 2026 . Published by Cold Spring Harbor Laboratory Press

LM622435 to E.P.N.), National Institutes of Health (NIH); the National Science Foundation (NSF EDGE 1923259 to C.E.S, U.F., and M.N.), and by NIH grant R35 GM138156 (to C.E.S.).

Author contributions: C.E.S., P.C., M.N., U.F, and A.D.B. conceived the study; C.E.S., E.S.C., and A.D.B. wrote the paper with revisions by G.Q-A., T.Q.D., D.D.J., E.P.N., T.G.W., O.S., M.N., and U.F.; J.M.G, S.M.S., and F. provided samples for sequencing; C.E.S., S.N.B., P.G., S.Koren, and A.P. performed whole genome and bulk and single-cell RNA-seq sequencing and assembly; C.E.S., A.-D.N., S.N.B., and P.G. built gene models and provided genome annotation; E.S.C., W.Y.W., and P.G. performed phylogenetic and orthology analyses; C.E.S., J.W., G.Q.A., J.G., D.D.J, B.B., and A.W. performed RNAseq and single-cell RNA-seq experiments and analysis; D.D.J., J.W., G.Q-A., and T.Q.D. performed ISH experiments and imaging; C.E.S, E.S.C, J.W., G.Q.A., W.Y.W., A-D.N., S.N.B., L.D., P.G., S.Koren, T.Q.D., E.P.N., S.Klasfeld, S.G.G., A.P., J.M., and O.S. processed raw data and conducted data analysis; A.-D.N., R.T.M., and T.G.W. contributed new analytic tools/resources and additional data.

REFERENCES

Beagley CT, Okimoto R, Wolstenholme DR. 1998. The mitochondrial genome of the sea anemone Metridium senile (Cnidaria): introns, a paucity of tRNA genes, and a near-standard genetic code. *Genetics* 148: 1091–108.

Benson G. 1999. Tandem repeats finder: a program to analyze DNA sequences. *Nucleic Acids Research* 27: 573–580.

Bermudez-Santana C, Attolini CS-O, Kirsten T, Engelhardt J, Prohaska SJ, Steigele S, Stadler PF. 2010. Genomic organization of eukaryotic tRNAs. *BMC Genomics* 11: 270.

Bradshaw B, Thompson K, Frank U. 2015. Distinct mechanisms underlie oral vs aboral regeneration in the cnidarian Hydractinia echinata ed. A. Sánchez Alvarado. *eLife* 4:

Downloaded from genome.cshlp.org on June 12, 2026 . Published by Cold Spring Harbor Laboratory Press

e05506.

Bridge D, Cunningham CW, Schierwater B, DeSalle R, Buss LW. 1992. Class-level relationships in the phylum Cnidaria: evidence from mitochondrial genome structure. *Proc Natl Acad Sci U S A* 89: 8750–3.

Brugler MR, France SC. 2007. The complete mitochondrial genome of the black coral Chrysopathes formosa (Cnidaria:Anthozoa:Antipatharia) supports classification of antipatharians within the subclass Hexacorallia. *Mol Phylogenet Evol* 42: 776–88.

Buchfink B, Xie C, Huson DH. 2015. Fast and sensitive protein alignment using DIAMOND. *Nature Methods* 12: 59–60.

Cartwright P, Collins A. 2007. Fossils and phylogenies: integrating multiple lines of evidence to investigate the origin of early major metazoan lineages. *Integrative and Comparative Biology* 47(5): 744-751.

Chan PP, Lin BY, Mak AJ, Lowe TM. 2021. tRNAscan-SE 2.0: improved detection and functional classification of transfer RNA genes. *Nucleic Acids Research* 49: 9077–9096.

Chapman JA, Kirkness EF, Simakov O, Hampson SE, Mitros T, Weinmaier T, Rattei T, Balasubramanian PG, Borman J, Busam D, et al. 2010. The dynamic genome of Hydra. *Nature* 464: 592–596.

Chari T, Weissbourd B, Gehring J, Ferraioli A, Leclère L, Herl M, Gao F, Chevalier S, Copley RR, Houliston E, Anderson, DJ, Pachter L. 2021. Whole-animal multiplexed single-cell RNA-seq reveals transcriptional shifts across *Clytia* medusa cell types. *Science Advances* 7:eabh1683.

Chen C, Chiou CY, Dai CF, Chen CA. 2008. Unique mitogenomic features in the scleractinian family pocilloporidae (scleractinia: astrocoeniina). *Mar Biotechnol (NY)* 10: 538–53.

Chen R, Sanders SM, Ma Z, Paschall J, Chang ES, Riscoe BM, Schnitzler CE, Baxevanis AD, Nicotra ML. 2023. XY sex determination in a cnidarian. *BMC Biology* 21: 32.

Chin C-S, Alexander DH, Marks P, Klammer AA, Drake J, Heiner C, Clum A, Copeland A,

Downloaded from genome.cshlp.org on June 12, 2026 . Published by Cold Spring Harbor Laboratory Press

907 Huddleston J, Eichler EE, et al. 2013. Nonhybrid, finished microbial genome assemblies
908 from long-read SMRT sequencing data. *Nature Methods* 10: 563–569.
909 Chin C-S, Peluso P, Sedlazeck FJ, Nattestad M, Concepcion GT, Clum A, Dunn C, O'Malley R,
910 Figueroa-Balderas R, Morales-Cruz A, et al. 2016. Phased diploid genome assembly
911 with single-molecule real-time sequencing. *Nat Methods* 13: 1050–1054.
912 Chiori R, Jager M, Denker E, Wincker P, Silva CD, Guyader HL, Manuel M, Quéinnec E. 2009.
913 Are Hox Genes Ancestrally Involved in Axial Patterning? Evidence from the Hydrozoan
914 Clytia hemisphaerica (Cnidaria). *PLOS ONE* 4: e4231.
915 Chourrout D, Delsuc F, Chourrout P, Edvardsen RB, Rentzsch F, Renfer E, Jensen MF, Zhu B,
916 de Jong P, Steele RE, et al. 2006. Minimal ProtoHox cluster inferred from bilaterian and
917 cnidarian Hox complements. *Nature* 442: 684–687.
918 Chrysostomou E, Flici H, Gornik SG, Salinas-Saavedra M, Gahan JM, McMahon ET, Thompson
919 K, Hanley S, Kincoyne M, Schnitzler CE, et al. 2022. A cellular and molecular analysis of
920 SoxB-driven neurogenesis in a cnidarian ed. M.E. Bronner. *eLife* 11: e78793.
921 Cloix C, Tutois S, Mathieu O, Cuvillier C, Espagnol MC, Picard G, Tourmente S. 2000. Analysis
922 of 5S rDNA Arrays in Arabidopsis thaliana: Physical Mapping and Chromosome-Specific
923 Polymorphisms. *Genome Res* 10: 679–690.
924 Darrow EM, Chadwick BP. 2014. A novel tRNA variable number tandem repeat at human
925 chromosome 1q23.3 is implicated as a boundary element based on conservation of a
926 CTCF motif in mouse. *Nucleic Acids Research* 42: 6421–6435.
927 De Bie T, Cristianini N, Demuth JP, Hahn MW. 2006. CAFE: a computational tool for the study
928 of gene family evolution. *Bioinformatics* 22: 1269–1271.
929 Derelle R, Momose T, Manuel M, Silva CD, Wincker P, Houliston E. 2010. Convergent origins
930 and rapid evolution of spliced leader trans-splicing in Metazoa: Insights from the
931 Ctenophora and Hydrozoa. *RNA* 16: 696–707.
932 D'Esposito M, Morelli F, Acampora D, Migliaccio E, Simeone A, Boncinelli E. 1991. EVX2, a

Downloaded from genome.cshlp.org on June 12, 2026 . Published by Cold Spring Harbor Laboratory Press

933 human homeobox gene homologous to the even-skipped segmentation gene, is
934 localized at the 5′ end of HOX4 locus on chromosome 2. *Genomics* 10: 43–50.
935 Driever W, Nüsslein-Volhard C. 1988. The bicoid protein determines position in the Drosophila
936 embryo in a concentration-dependent manner. *Cell* 54: 95–104.
937 Duboule D. 2007. The rise and fall of Hox gene clusters. *Development* 134: 2549–2560.
938 DuBuc TQ, Ryan JF, Shinzato C, Satoh N, Martindale MQ. 2012. Coral Comparative Genomics
939 Reveal Expanded Hox Cluster in the Cnidarian–Bilaterian Ancestor. *Integrative and*
940 *Comparative Biology* 52: 835–841.
941 DuBuc TQ, Schnitzler CE, Chrysostomou E, McMahon ET, Febrimarsa, Gahan JM, Buggie T,
942 Gornik SG, Hanley S, Barreira SN, et al. 2020. Transcription factor AP2 controls
943 cnidarian germ cell induction. *Science* 367: 757–762.
944 Emms DM, Kelly S 2019. OrthoFinder: phylogenetic orthology inference for comparative
945 genomics. *Genome Biology* 20: 238.
946 English AC, Richards S, Han Y, Wang M, Vee V, Qu J, Qin X, Muzny DM, Reid JG, Worley KC,
947 et al. 2012. Mind the Gap: Upgrading Genomes with Pacific Biosciences RS Long-Read
948 Sequencing Technology. *PLOS ONE* 7: e47768.
949 Faiella A, D'Esposito M, Rambaldi M, Acampora D, Balsfiore S, Stornaiuolo A, Mallamaci A,
950 Migliaccio E, Gulisano M, Simeone A, et al. 1991. Isolation and mapping of EVx1, a
951 human homeobox gene homologus to even-skipped, localized at the 5′ end of Hox1
952 locus on chromosome 7. *Nucleic Acids Research* 19: 6541–6545.
953 Friedländer MR, Mackowiak SD, Li N, Chen W, Rajewsky N. 2012. miRDeep2 accurately
954 identifies known and hundreds of novel microRNA genes in seven animal clades.
955 *Nucleic Acids Research* 40: 37–52.
956 Gahan JM, Cartwright P, Nicotra ML, Schnitzler CE, Steinmetz PRH, Juliano CE. 2023.
957 Cnidofest 2022: hot topics in cnidarian research. EvoDevo 14:13.
958 Gold DA, Katsuki T, Li Y, Yan X, Regulski M, Ibberson D, Holstein T, Steele RE, Jacobs DK,

Downloaded from genome.cshlp.org on June 12, 2026 . Published by Cold Spring Harbor Laboratory Press

959 Greenspan RJ. 2019. The genome of the jellyfish Aurelia and the evolution of animal
960 complexity. *Nature Ecology & Evolution* 3: 96–104.
961 Guo L, Accorsi A, He S, Guerrero-Hernández C, Sivagnanam S, McKinney S, Gibson M,
962 Sánchez Alvarado A. 2018. An adaptable chromosome preparation methodology for use
963 in invertebrate research organisms. *BMC Biol* 16: 25.
964 Haas BJ, Salzberg SL, Zhu W, Pertea M, Allen JE, Orvis J, White O, Buell CR, Wortman JR.
965 2008. Automated eukaryotic gene structure annotation using EVidenceModeler and the
966 Program to Assemble Spliced Alignments. *Genome Biol* 9: R7.
967 Han MV, Thomas GWC, Lugo-Martinez J, Hahn MW. 2013. Estimating Gene Gain and Loss
968 Rates in the Presence of Error in Genome Assembly and Annotation Using CAFE 3.
969 *Molecular Biology and Evolution* 30: 1987–1997.Hare EE, Johnston JS. 2011. Genome
970 Size Determination Using Flow Cytometry of Propidium Iodide-Stained Nuclei. In
971 *Molecular Methods for Evolutionary Genetics* (eds. V. Orgogozo and M.V. Rockman),
972 *Methods in Molecular Biology*, pp. 3–12, Humana Press, Totowa, NJ
973 https://doi.org/10.1007/978-1-61779-228-1_1 (Accessed May 4, 2021).
974 Hastings KEM. 2005. SL trans-splicing: easy come or easy go? *Trends in Genetics* 21: 240–
975 247.
976 Holland PW, Booth HAF, Bruford EA. 2007. Classification and nomenclature of all human
977 homeobox genes. *BMC Biology* 5: 47.
978 Holland PWH. 2013. Evolution of homeobox genes. *WIREs Developmental Biology* 2: 31–45.
979 Huene AL, Sanders SM, Ma Z, Nguyen A-D, Koren S, Michaca MH, Mullikin JC, Phillippy AM,
980 Schnitzler CE, Baxevanis AD, et al. 2022. A family of unusual immunoglobulin
981 superfamily genes in an invertebrate histocompatibility complex. *Proceedings of the*
982 *National Academy of Sciences* 119: e2207374119.
983 Hwang JS, Takaku Y, Chapman J, Ikeo K, David CN, Gojobori T. 2008. Cilium Evolution:
984 Identification of a Novel Protein, Nematocilin, in the Mechanosensory Cilium of Hydra

Downloaded from genome.cshlp.org on June 12, 2026 . Published by Cold Spring Harbor Laboratory Press

985 Nematocytes. *Molecular Biology and Evolution* 25: 2009–2017.
986 Jeon Y, Park SG, Lee N, Weber JA, Kim H-S, Hwang S-J, Woo S, Kim H-M, Bhak Y, Jeon S, et
987 al. 2019. The Draft Genome of an Octocoral, Dendronephthya gigantea. *Genome*
988 *Biology and Evolution* 11: 949–953.
989 Kalvari I, Argasinska J, Quinones-Olvera N, Nawrocki EP, Rivas E, Eddy SR, Bateman A, Finn
990 RD, Petrov AI. 2018. Rfam 13.0: shifting to a genome-centric resource for non-coding
991 RNA families. *Nucleic Acids Research* 46: D335–D342.
992 Kayal E, Bentlage B, Cartwright P, Yanagihara AA, Lindsay DJ, Hopcroft RR, Collins AG. 2015.
993 Phylogenetic analysis of higher-level relationships within Hydroidolina (Cnidaria:
994 Hydrozoa) using mitochondrial genome data and insight into their mitochondrial
995 transcription. *PeerJ* 3: e1403.
996 Kayal E, Bentlage B, Collins AG, Kayal M, Pirro S, Lavrov DV. 2012. Evolution of linear
997 mitochondrial genomes in medusozoan cnidarians. *Genome Biol Evol* 4: 1–12.
998 Kayal E, Lavrov DV. 2008. The mitochondrial genome of Hydra oligactis (Cnidaria, Hydrozoa)
999 sheds new light on animal mtDNA evolution and cnidarian phylogeny. *Gene* 410: 177–
1000 86.
1001 Khalturin K, Shinzato C, Khalturina M, Hamada M, Fujie M, Koyanagi R, Kanda M, Goto H,
1002 Anton-Erxleben F, Toyokawa M, et al. 2019. Medusozoan genomes inform the evolution
1003 of the jellyfish body plan. *Nature Ecology & Evolution* 3: 811–822.
1004 Klug M, Tardent P, Smid I, Holstein T. 1984. Presence and localization of chitinase in Hydra and
1005 Podocoryne (Cnidaria, Hydrozoa). *Journal of Experimental Zoology* 229: 69–72.
1006 Kon-Nanjo K, Kon T, Horkan HR, Febrimarsa, Steele RE, Cartwright P, Frank U, Simakov O.
1007 2023. Chromosome-level genome assembly of Hydractinia symbiolongicarpus. G3
1008 Genes|Genomes|Genetics 13: jkad107.
1009 Koren S, Walenz BP, Berlin K, Miller JR, Bergman NH, Phillippy AM. 2017. Canu: scalable and
1010 accurate long-read assembly via adaptive k-mer weighting and repeat separation.

Downloaded from genome.cshlp.org on June 12, 2026 . Published by Cold Spring Harbor Laboratory Press

Genome Res 27: 722–736.

Kurtz S, Phillippy A, Delcher AL, Smoot M, Shumway M, Antonescu C, Salzberg SL. 2004. Versatile and open software for comparing large genomes. *Genome Biol* 5: R12.

Leclère L, Horin C, Chevalier S, Lapébie P, Dru P, Peron S, Jager M, Condamine T, Pottin K, Romano S, et al. 2019. The genome of the jellyfish Clytia hemisphaerica and the evolution of the cnidarian life-cycle. *Nature Ecology & Evolution* 3: 801–810.

Long EO, Dawid IB. 1980. Repeated Genes in Eukaryotes. *Annual Review of Biochemistry* 49: 727–764.

Maxwell EK, Schnitzler CE, Havlak P, Putnam NH, Nguyen A-D, Moreland RT, Baxevanis AD. 2014. Evolutionary profiling reveals the heterogeneous origins of classes of human disease genes: implications for modeling disease genetics in animals. *BMC Evol Biol* 14: 212.

Mendivil Ramos O, Barker D, Ferrier DEK. 2012. Ghost Loci Imply Hox and ParaHox Existence in the Last Common Ancestor of Animals. *Current Biology* 22: 1951–1956.

Moran Y, Praher D, Fredman D, Technau U. 2013. The Evolution of MicroRNA Pathway Protein Components in Cnidaria. *Molecular Biology and Evolution* 30: 2541–2552.

Munro C, Cadis H, Pagnotta S, Houliston E, Huynh J-R. 2023. Conserved meiotic mechanisms in the cnidarian Clytia hemisphaerica revealed by Spo11 knockout. *Science Advances* 9: eadd2873.

Nawrocki EP, Eddy SR. 2013. Infernal 1.1: 100-fold faster RNA homology searches. *Bioinformatics* 29: 2933–2935.

Nicotra ML. 2019. Invertebrate allorecognition. *Current Biology* 29: R463–R467.

Nicotra ML, Powell AE, Rosengarten RD, Moreno M, Grimwood J, Lakkis FG, Dellaporta SL, Buss LW. 2009. A Hypervariable Invertebrate Allodeterminant. *Current Biology* 19: 583–589.

Nong W, Cao J, Li Y, Qu Z, Sun J, Swale T, Yip HY, Qian PY, Qiu JW, Kwan HS, et al. 2020.

Downloaded from genome.cshlp.org on June 12, 2026 . Published by Cold Spring Harbor Laboratory Press

Jellyfish genomes reveal distinct homeobox gene clusters and conservation of small RNA processing. *Nat Commun* 11: 3051.

Pearson JC, Lemons D, McGinnis W. 2005. Modulating Hox gene functions during animal body patterning. *Nat Rev Genet* 6: 893–904.

Praher D, Zimmermann B, Dnyansagar R, Miller DJ, Moya A, Modepalli V, Fridrich A, Sher D, Friis-Møller L, Sundberg P, et al. 2021. Conservation and turnover of miRNAs and their highly complementary targets in early branching animals. *Proceedings of the Royal Society B: Biological Sciences* 288: 20203169.

Procino A. 2016. Class I Homeobox Genes, “The Rosetta Stone of the Cell Biology”, in the Regulation of Cardiovascular Development. *Current Medicinal Chemistry* 23: 265–275.

Putnam NH, O’Connell BL, Stites JC, Rice BJ, Blanchette M, Calef R, Troll CJ, Fields A, Hartley PD, Sugnet CW, et al. 2016. Chromosome-scale shotgun assembly using an in vitro method for long-range linkage. *Genome Res* 26: 342–350.

Putnam NH, Srivastava M, Hellsten U, Dirks B, Chapman J, Salamov A, Terry A, Shapiro H, Lindquist E, Kapitonov VV, et al. 2007. Sea Anemone Genome Reveals Ancestral Eumetazoan Gene Repertoire and Genomic Organization. *Science* 317: 86–94.

R Core Team 2021. R: A language and environment for statistical computing. R Foundation for Statistical Computing, Vienna, Austria. https://www.R-project.org.Rosa SFP, Powell AE, Rosengarten RD, Nicotra ML, Moreno MA, Grimwood J, Lakkis FG, Dellaporta SL, Buss LW. 2010. Hydractinia Allodeterminant alr1 Resides in an Immunoglobulin Superfamily-like Gene Complex. *Current Biology* 20: 1122–1127.

Ruperti F, Papadopoulos N, Musser JM, Mirdita M, Steinegger M, Arendt D. 2023. Cross-phyla protein annotation by structural prediction and alignment. *Genome Biology* 24: 113.

Ryan JF, Burton PM, Mazza ME, Kwong GK, Mullikin JC, Finnerty JR. 2006. The cnidarian-bilaterian ancestor possessed at least 56 homeoboxes: evidence from the starlet sea anemone, Nematostella vectensis. *Genome Biol* 7: R64.

Downloaded from genome.cshlp.org on June 12, 2026 . Published by Cold Spring Harbor Laboratory Press

1063 Sanderson MJ. 2003. r8s: inferring absolute rates of molecular evolution and divergence times
1064 in the absence of a molecular clock. *Bioinformatics* 19: 301–302.
1065 Satija R, Farrell JA, Gennert D, Schier AF, Regev A. 2015. Spatial reconstruction of single-cell
1066 gene expression data. *Nature Biotechnology* 33: 495–502.
1067 Schulte D, Frank D. 2014. TALE transcription factors during early development of the vertebrate
1068 brain and eye. *Developmental Dynamics* 243: 99–116.
1069 Sebé-Pedrós A, Saudemont B, Chomsky E, Plessier F, Mailhé M-P, Renno J, Loe-Mie Y,
1070 Lifshitz A, Mukamel Z, Schmutz S, et al. 2018. Cnidarian cell type diversity and
1071 regulation revealed by whole-organism single-cell RNA-seq. *Cell* 173: 1520-1534.e20.
1072 Siebert S, Farrell JA, Cazet JF, Abeykoon Y, Primack AS, Schnitzler CE, Juliano CE. 2019.
1073 Stem cell differentiation trajectories in *Hydra* resolved at single-cell resolution. *Science*
1074 365: eaav9314.
1075 Shao Z, Graf S, Chaga OY, Lavrov DV. 2006. Mitochondrial genome of the moon jelly Aurelia
1076 aurita (Cnidaria, Scyphozoa): A linear DNA molecule encoding a putative DNA-
1077 dependent DNA polymerase. *Gene* 381: 92–101.
1078 Simakov O, Bredeson J, Berkoff K, Marletaz F, Mitros T, Schultz DT, O'Connell BL, Dear P,
1079 Martinez DE, Steele RE, et al. 2022. Deeply conserved synteny and the evolution of
1080 metazoan chromosomes. *Science Advances* 8: eabi5884.
1081 Simão FA, Waterhouse RM, Ioannidis P, Kriventseva EV, Zdobnov EM. 2015. BUSCO:
1082 assessing genome assembly and annotation completeness with single-copy orthologs.
1083 *Bioinformatics* 31: 3210–3212.
1084 Smith DR, Kayal E, Yanagihara AA, Collins AG, Pirro S, Keeling PJ. 2012. First complete
1085 mitochondrial genome sequence from a box jellyfish reveals a highly fragmented linear
1086 architecture and insights into telomere evolution. *Genome Biol Evol* 4: 52–8.
1087 Song S, Jiang F, Yuan J, Guo W, Miao Y. 2013. Exceptionally high cumulative percentage of
1088 NUMTs originating from linear mitochondrial DNA molecules in the Hydra magnipapillata

Downloaded from genome.cshlp.org on June 12, 2026 . Published by Cold Spring Harbor Laboratory Press

1089 genome. *BMC Genomics* 14: 447.
1090 Stampar SN, Broe MB, Macrander J, Reitzel AM, Brugler MR, Daly M. 2019. Linear
1091 Mitochondrial Genome in Anthozoa (Cnidaria): A Case Study in Ceriantharia. *Sci Rep* 9:
1092 6094.
1093 Steele RE, David CN, Technau U. 2011. A genomic view of 500 million years of cnidarian
1094 evolution. *Trends in Genetics* 27: 7–13.
1095 Steinworth BM, Martindale MQ, Ryan JF. 2023. Gene Loss may have Shaped the Cnidarian
1096 and Bilaterian Hox and ParaHox Complement ed. S.F. Valverde. *Genome Biology and*
1097 *Evolution* 15: evac172.
1098 Stover NA, Steele RE. 2001. Trans-spliced leader addition to mRNAs in a cnidarian. *PNAS* 98:
1099 5693–5698.
1100 Tawari B, Ali IKM, Scott C, Quail MA, Berriman M, Hall N, Clark CG. 2008. Patterns of Evolution
1101 in the Unique tRNA Gene Arrays of the Genus Entamoeba. *Molecular Biology and*
1102 *Evolution* 25: 187–198.
1103 Török A, Schiffer PH, Schnitzler CE, Ford K, Mullikin JC, Baxevanis AD, Bacic A, Frank U,
1104 Gornik SG. 2016. The cnidarian Hydractinia echinata employs canonical and highly
1105 adapted histones to pack its DNA. *Epigenetics & Chromatin* 9: 36.
1106 Törönen P, Medlar A, Holm L. 2018. PANNZER2: a rapid functional annotation web server.
1107 *Nucleic Acids Research* 46: W84–W88.
1108 Varley Á, Horkan HR, McMahon ET, Krasovec G, Frank U. 2023. Pluripotent, germ cell
1109 competent adult stem cells underlie cnidarian regenerative ability and clonal growth.
1110 *Current Biology* 33: 1–10.
1111 Voigt O, Erpenbeck D, Worheide G. 2008. A fragmented metazoan organellar genome: the two
1112 mitochondrial chromosomes of Hydra magnipapillata. *BMC Genomics* 9: 350.
1113 Wagner DE, Wang IE, Reddien PW. 2011. Clonogenic Neoblasts Are Pluripotent Adult Stem
1114 Cells That Underlie Planarian Regeneration. *Science* 332: 811–816.

Downloaded from genome.cshlp.org on June 12, 2026 . Published by Cold Spring Harbor Laboratory Press

Walker BJ, Abeel T, Shea T, Priest M, Abouelliel A, Sakthikumar S, Cuomo CA, Zeng Q, Wortman J, Young SK, et al. 2014. Pilon: An Integrated Tool for Comprehensive Microbial Variant Detection and Genome Assembly Improvement. *PLOS ONE* 9: e112963.

Wang D, King SM, Quill TA, Doolittle LK, Garbers DL. 2003. A new sperm-specific Na + /H + Exchanger required for sperm motility and fertility. *Nature Cell Biology* 5: 1117–1122.

Wang J, Sun H, Jiang M, Li J, Zhang P, Chen H, Mei Y, Fei L, Lai S, Han X, et al. 2021. Tracing cell-type evolution by cross-species comparison of cell atlases. *Cell Reports* 34: 108803.

Weismann A. 1883. Die Entstehung der Sexualzellen bei Hydromedusen (The origin of the sexual cells in hydromedusae). Gustav Fischer-Verlag, Jena.

Wessel GM. 2013. Getting schooled the ol'fashioned way. August Weismann and the "germ terms." *Molecular Reproduction and Development* 80. https://onlinelibrary.wiley.com/doi/abs/10.1002/mrd.22149 (Accessed May 3, 2021).

Wheeler BM, Heimberg AM, Moy VN, Sperling EA, Holstein TW, Heber S, Peterson KJ. 2009. The deep evolution of metazoan microRNAs. *Evolution & Development* 11: 50–68.

Wong WY, Simakov O, Bridge DM, Cartwright P, Bellantuono AJ, Kuhn A, Holstein TW, David CN, Steele RE, Martínez DE. 2019. Expansion of a single transposable element family is associated with genome-size increase and radiation in the genus Hydra. *Proceedings of the National Academy of Sciences* 116: 22915–22917.

Young RA. 2011. Control of the Embryonic Stem Cell State. *Cell* 144: 940–954.

Zacharias H, Anokhin B, Khalturin K, Bosch TCG. 2004. Genome sizes and chromosomes in the basal metazoan Hydra. *Zoology* 107: 219–227.

Zimmermann B, Montenegro, JD, Robb SMC, Fropf WJ, Weilguny L, He S, Chen S, Lovegrove-Walsh J, Hill EM, Chen C-Y, Ragkousi K, Praher D, Fredman D, Shultz D, Moran Y, Simakov O, Genikhovich G, Gibson MC, Technau U. 2023. Topological structures and syntenic conservation in sea anemone genomes. *Nature Communications* 14: 8270.

Downloaded from genome.cshlp.org on June 12, 2026 . Published by Cold Spring Harbor Laboratory Press

Figure 1. Overview of *Hydractinia*, phylogenetic analysis, synteny analysis, and analysis of repetitive elements. (A) *Hydractinia echinata* colony (top panel); *Hydractinia symbiolongicarpus* colony (bottom panel). (B) Maximum likelihood phylogeny estimated from a data set of single copy orthologs as inferred by OrthoFinder2 showing that the two *Hydractinia* species cluster together with *C. hemisphaerica* and *H. vulgaris* branching next to them within the Hydrozoa. Divergence times were estimated using the r8s program (Sanderson 2003). The age of Cnidaria was fixed at 570 MYA and the age of Hydrozoa constrained to 500 MYA based upon Cartwright and Collins (2007). (C) Syntenic dot plots comparing *H. symbiolongicarpus* with four cnidarian species: *H. echinata*; *C. hemisphaerica; H. vulgaris*; and *N. vectensis*. Colored boxes indicate linkage groups. (D) Stacked bar chart showing proportions of different transposable elements classes in each *Hydractinia* genome using RepeatMasker *de novo* analysis. “ARTEFACT” refers to elements often found in cloning vectors that may contaminate sequencing projects. (E) Repeat landscape analysis showing overall a highly similar evolutionary history of invasion of repetitive elements in the two species. In *H. symbiolongicarpus*, there was a species-specific recent expansion (at approximately 10% nucleotide substitution) of LTR retrotransposons.

Downloaded from genome.cshlp.org on June 12, 2026 . Published by Cold Spring Harbor Laboratory Press

Figure 2. Summary of orthogroup evolution across a subset of sampled taxa. Left: Changes in gene family size estimated using CAFE. Pie charts represent changes along the branch leading to a given node or tip for all 8,433 orthogroups inferred to be present in the common ancestor of this tree. Branch lengths are as depicted in Fig. 1B. Right: Proportion of input proteome sequences assigned by OrthoFinder to different orthogroup categories. See Supplemental Fig. S16 for results for every species included in the OrthoFinder analysis and Supplemental Table S12 tab SM1 for the number of input sequences in each proteome. The data used to create these figures can be found in Supplemental Table S12 tabs X.2-3. *A. aurita* Pacific genome from Gold et al. 2019, Baltic/Atlantic genome from Khalturin et al. 2019.

Downloaded from genome.cshlp.org on June 12, 2026 . Published by Cold Spring Harbor Laboratory Press

Figure 3. Genomic organization of Hox and ParaHox genes in five cnidarian genomes. Solid lines sharing homeobox genes represent genomic scaffolds. Scaffold and gene ID numbering in *Hydractinia* genomes is shown above gene boxes. Broken lines depict homologous cnidarian-specific Hox genes. Alternative gene names are shown above gene boxes for *C. hemisphaerica*, *N. vectensis*, and *A. digitifera*.

Downloaded from genome.cshlp.org on June 12, 2026 . Published by Cold Spring Harbor Laboratory Press

Figure 4. *Hydractinia* single-cell atlas represented as a labeled UMAP and validation of several cell type markers using fluorescent *in situ* hybridization (FISH). (A) *Hydractinia* single-cell atlas UMAP with 18 clusters (C0-C17). (B-F) UMAP expression of select marker genes (left panels) and spatial expression pattern of marker gene in polyps via FISH (right panel). Blue staining = Hoechst, Pink = marker gene. *Piwi1* (B) and *PCNA* (C) expression in the i-cell band in the middle of the body column of a feeding polyp. (D) *Ncol1* expression in nematoblasts in the lower body column of a feeding polyp. (E) *SLC9C1* expression in mature sperm cells in gonads of male sexual polyps. (F) *Nematocilin A* expression in a subset of nematocytes in the tentacles of a feeding polyp. Close-up view of tentacles in panels 3 and 4 both show higher magnification images from the same polyp as in panel 2, showing expression is specific to cnidocytes. Panel 4 adds DIC. (G) *ARSTNd2-like* expression in a subset of nematocytes in the body column of a feeding polyp. Panels 3 and 4 both show higher magnification images from the same polyp as in panel 2, showing expression is specific to cnidocytes. Panel 4 adds DIC. (H) *Chitinase 1* expression in gland cells in the endodermal epithelial cell layer of a feeding polyp. Panel 3 and 4 both show higher magnification images from the same polyp as in panel 2, showing expression is specific to gland cells. Panel 4 adds DIC. All images shown were projected from confocal stacks. All scale bars = 100 µm. Abbreviations in (A): ecEP: ectodermal epithelial cell, enEP: endodermal epithelial cell, germ: germ cell, ISC: interstitial stem cell, Mgc: mucous gland cell, nb: nematoblast, nem: nematocyte, prog: progenitor, sprm: sperm, Zgc: zymogen gland cell.

Downloaded from genome.cshlp.org on June 12, 2026 . Published by Cold Spring Harbor Laboratory Press

Figure 5. Results from the lineage-specificity analysis using OrthoFinder results and the UMAP cluster marker genes. (A) Stacked bar chart showing the percentage of *H. symbiolongicarpus* single-cell atlas cluster markers shared among animal phyla. The bottom legend shows eight different categories, dividing the markers into different groups depending on how the orthologs are shared among the species. The “Not assigned to orthogroup" category represents markers that could not be placed into an orthogroup. The other categories are markers that have at least one homolog between *H. symbiolongicarpus* and that category, except for the “Symbio-specific” category which represents markers that fell into orthogroups containing only *H. symbiolongicarpus* genes. For example, hypothetical marker gene A from *H. symbiolongicarpus* would be an “Other multispecies orthogroup” marker if it was found in *H. symbiolongicarpus* and at least one animal outside of cnidaria, but it would be a “Cnidarian-specific” marker if it was found in *H. symbiolongicarpus* and at least one cnidarian outside the Medusozoa. Stacked bars represent the seven major cell types split into nine groups, followed by all individual clusters, and finally the total genes expressed in the *Hydractinia* single-cell dataset (16,069 genes) and total genes predicted from the *Hydractinia* genome (22,022 genes). The marker gene count bars on the right indicate how many markers are present in each major cell type and cluster. (B) Histogram dividing the 317 orthogroup-assigned i-cell (clusters 6 and 7) markers by how many are shared by a given number of species. Legend is the same as for panel A but the following categories are excluded from this chart: unassigned genes (two genes) and *H. symbiolongicarpus*-specific genes (none).

Downloaded from genome.cshlp.org on June 12, 2026 . Published by Cold Spring Harbor Laboratory Press

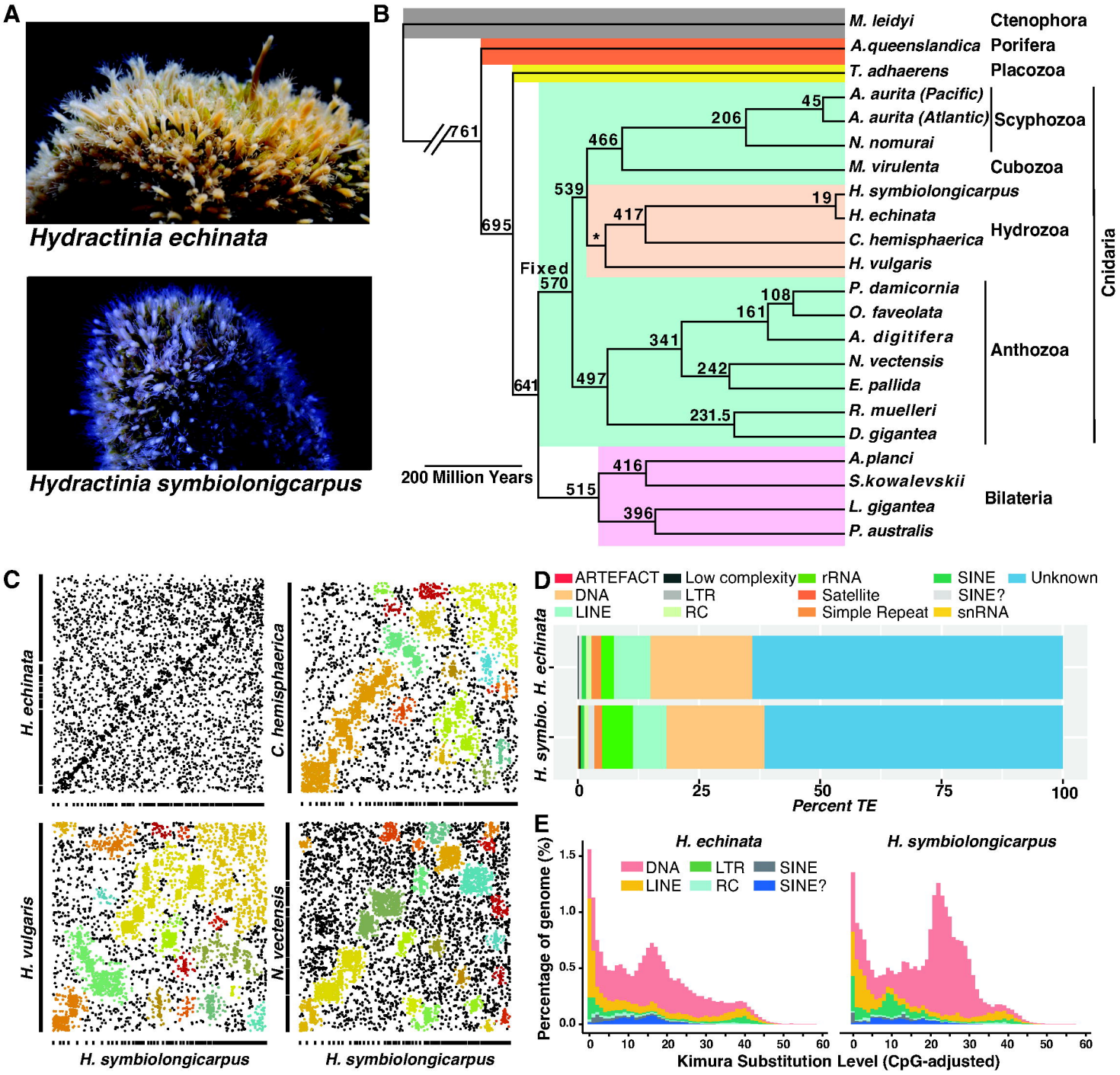

Downloaded from genome.cshlp.org on June 12, 2026 . Published by Cold Spring Harbor Laboratory Press

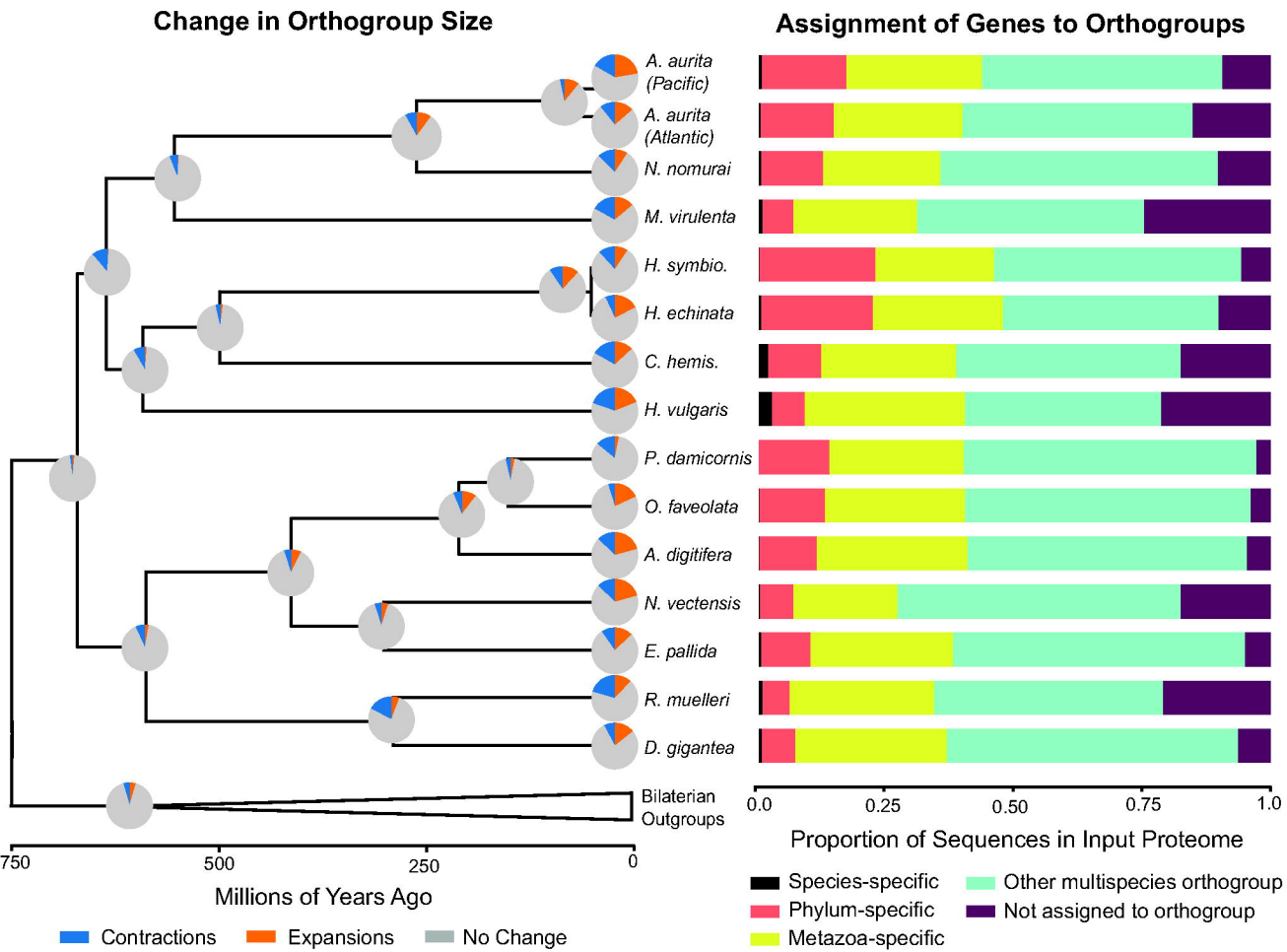

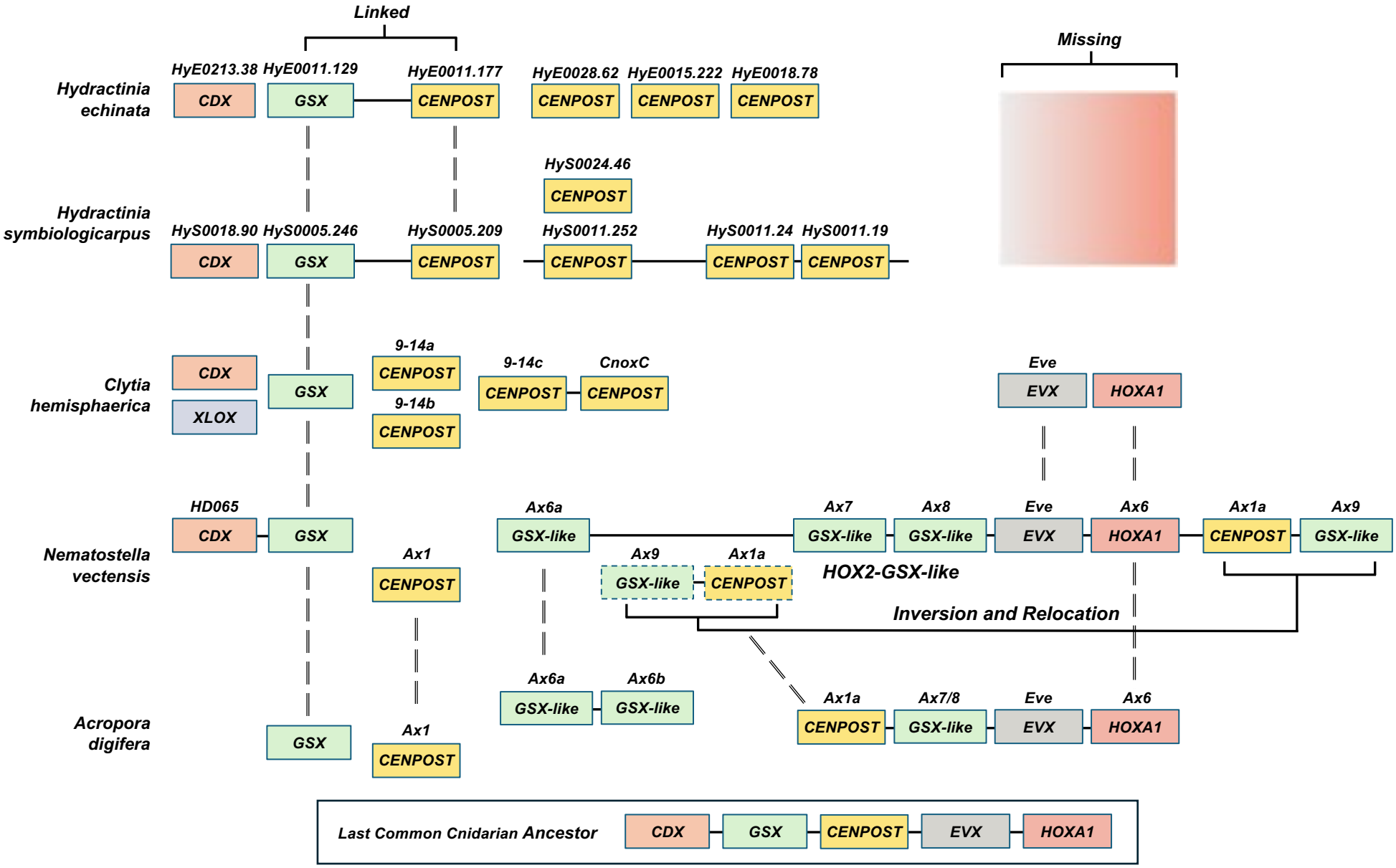
Linked
Missing
Hydractinia echinata
HyE0213.38
HyE0011.129
HyE0011.177
HyE0028.62
HyE0015.222
HyE0018.78
CDX
GSX
CENPOST
CENPOST
CENPOST
CENPOST
Hydractinia symbiologicarpus
HyS0024.46
CENPOST
HyS0018.90
HyS0005.246
HyS0005.209
HyS0011.252
HyS0011.24
HyS0011.19
CDX
GSX
CENPOST
CENPOST
CENPOST
CENPOST
Clytia hemisphaerica
CDX
XLOX
GSX
9-14a
CENPOST
9-14b
CENPOST
9-14c
CENPOST
CnoxC
CENPOST
Eve
EVX
HOXA1
Nematostella vectensis
HD065
CDX
GSX
Ax1
CENPOST
Ax6a
GSX-like
Ax9
GSX-like
Ax1a
CENPOST
Ax7
GSX-like
Ax8
GSX-like
Eve
EVX
Ax6
HOXA1
Ax1a
CENPOST
Ax9
GSX-like
HOX2-GSX-like
Inversion and Relocation
Acropora digifera
GSX
Ax1
CENPOST
Ax6a
GSX-like
Ax6b
GSX-like
Ax1a
CENPOST
Ax7/8
GSX-like
Eve
EVX
Ax6
HOXA1
Last Common Cnidarian Ancestor
CDX
GSX
CENPOST
EVX
HOXA1

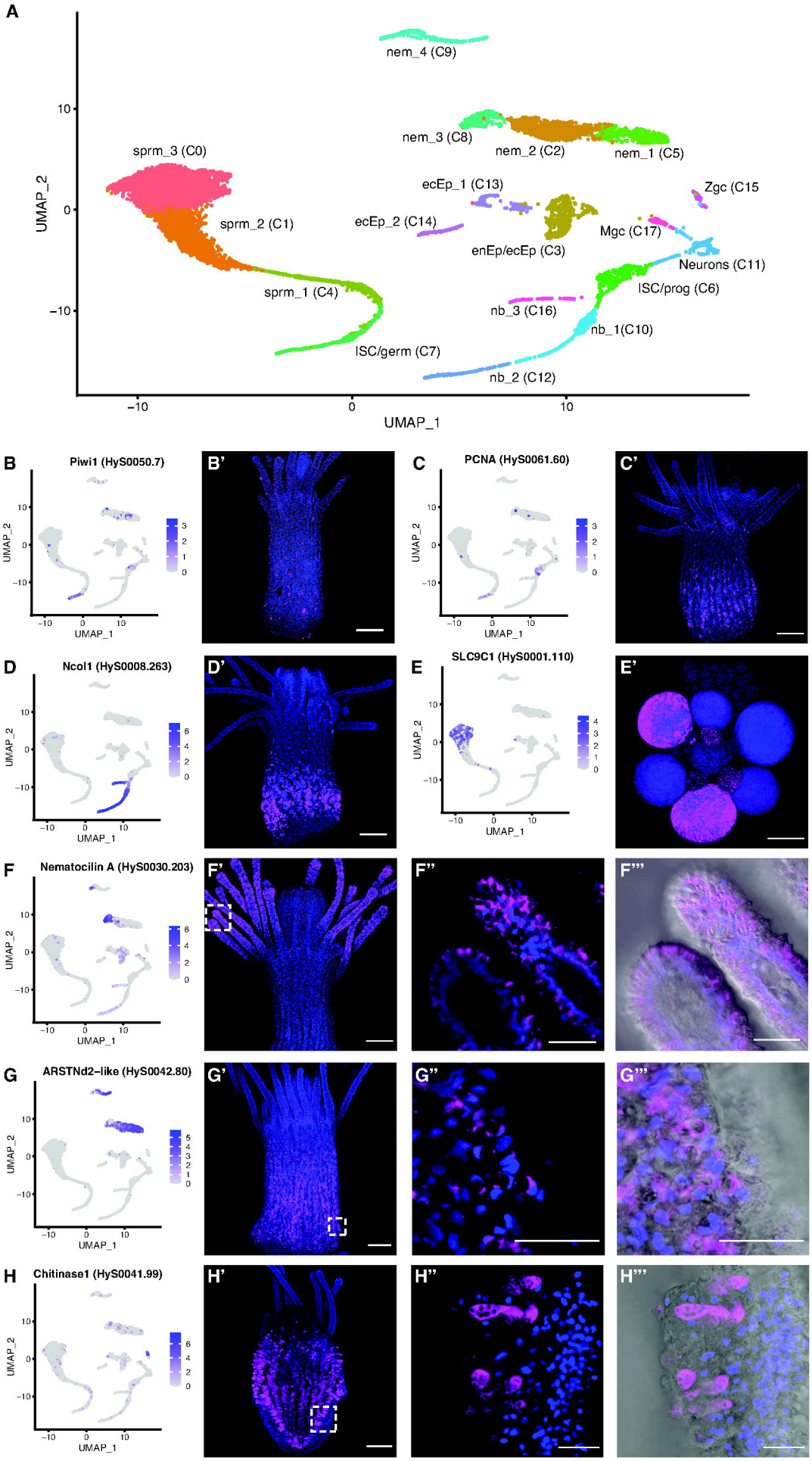
A
nem_4 (C9)
nem_3 (C8)
nem_2 (C2)
nem_1 (C5)
sprm_3 (C0)
sprm_2 (C1)
sprm_1 (C4)
ISC/germ (C7)
ecEp_1 (C13)
ecEp_2 (C14)
enEp/ecEp (C3)
Zgc (C15)
Mgc (C17)
Neurons (C11)
ISC/prog (C6)
nb_3 (C16)
nb_1(C10)
nb_2 (C12)
UMAP_1
UMAP_2
B
Piwi1 (HyS0050.7)
B'
C
PCNA (HyS0061.60)
C'
D
Ncol1 (HyS0008.263)
D'
E
SLC9C1 (HyS0001.110)
E'
F
Nematocilin A (HyS0030.203)
F'
F''
F'''
G
ARSTNd2–like (HyS0042.80)
G'
G''
G'''
H
Chitinase1 (HyS0041.99)
H'
H''
H'''

A

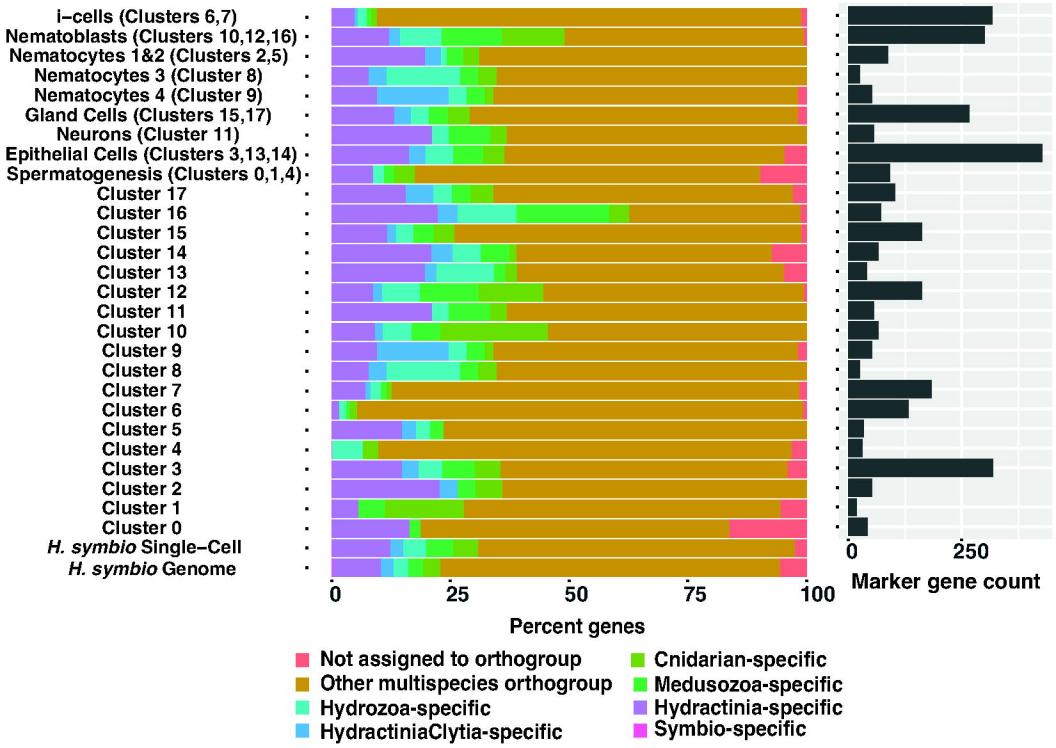
i–cells (Clusters 6,7)
Nematoblasts (Clusters 10,12,16)
Nematocytes 1&2 (Clusters 2,5)
Nematocytes 3 (Cluster 8)
Nematocytes 4 (Cluster 9)
Gland Cells (Clusters 15,17)
Neurons (Cluster 11)
Epithelial Cells (Clusters 3,13,14)
Spermatogenesis (Clusters 0,1,4)
Cluster 17
Cluster 16
Cluster 15
Cluster 14
Cluster 13
Cluster 12
Cluster 11
Cluster 10
Cluster 9
Cluster 8
Cluster 7
Cluster 6
Cluster 5
Cluster 4
Cluster 3
Cluster 2
Cluster 1
Cluster 0
H. symbio Single–Cell
H. symbio Genome
0
25
50
75
100
Percent genes
0
250
Marker gene count
Not assigned to orthogroup
Other multispecies orthogroup
Hydrozoa-specific
HydractiniaClytia-specific
Cnidarian-specific
Medusozoa-specific
Hydractinia-specific
Symbio-specific

B

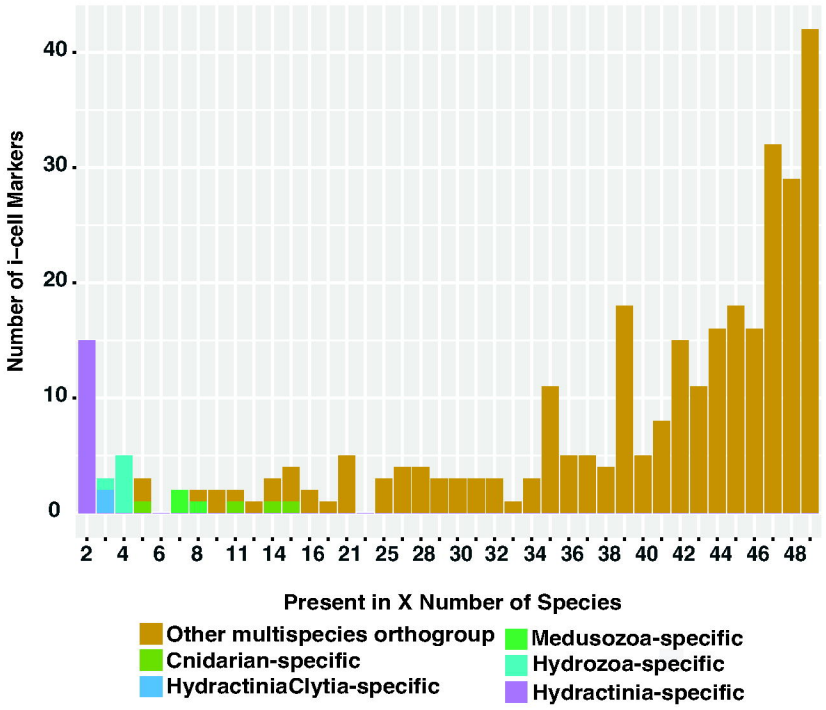
Number of i–cell Markers
40
30
20
10
0
2
4
6
8
11
14
16
21
25
28
30
32
34
36
38
40
42
44
46
48
Present in X Number of Species
Other multispecies orthogroup
Cnidarian-specific
HydractiniaClytia-specific
Medusozoa-specific
Hydrozoa-specific
Hydractinia-specific